

Published in final edited form as:

Dalton Trans. 2015 March 21; 44(11): 4819–4844. doi:10.1039/c4dt02846e.

A nuclear chocolate box: the periodic table of nuclear medicine

P. J. Blower^a

^aKing's College London, Division of Imaging Sciences and Biomedical Engineering, 4th Floor Lambeth Wing, St Thomas' Hospital, London SE1 7EH

Abstract

Radioisotopes of elements from all parts of the periodic table find both clinical and research applications in radionuclide molecular imaging and therapy (nuclear medicine). This article provides an overview of these applications in relation to both the radiological properties of the radionuclides and the chemical properties of the elements, indicating past successes, current applications and future opportunities and challenges for inorganic chemistry.

Introduction

Since the first experimental use of the beta-emitting cyclotron-produced radionuclide phosphorus-32 for treatment of patients with haematological disease in the 1930s, the use of radioisotopes in medicine has expanded into a mainstream clinical speciality incorporating both diagnostic imaging (exploiting the tissue penetration of gamma rays derived from nuclear decay or positron annihilation) and targeted therapy (exploiting the cellular toxicity of non-penetrating alpha and beta particles and secondary electrons). Via landmark steps including clinical use of iodine-131 for therapy and diagnosis of thyroid disease, and key technologies such as the Anger gamma camera and, later, single-photon emission tomography (SPET), the technetium-99m generator, positron emission tomography (PET) and medical cyclotrons, radioisotope imaging has evolved into today's set of cutting-edge technologies with applications and instrumentation dedicated not only to clinical medicine but to basic biomedical and preclinical research. Over this time the range of available radioisotopes, produced by cyclotrons, nuclear reactors and generators, has grown and now represents all areas of the periodic table with applications that have evolved to make best use of both the radiological (half-life, specific activity and of course emission type – alpha, beta, gamma, positron, Auger electron, and even associated Cerenkov light emission) and chemical properties (biological behaviour and chemical suitability for incorporation into complex targeting molecules and bioconjugates) of the radioelement for the biomedical purpose at hand. This article presents a survey of the variety of these properties and their uses, linking properties to applications and briefly reporting on current developments and future challenges for inorganic chemists in this field, using the Periodic Table (Fig. 1) – the “nuclear chocolate box”, from which selections can be made to suit a variety of different needs - as a basis of classification. In this way it is hoped that the article will provide a map for navigation of radionuclide imaging and therapy specifically for inorganic chemists. It should indicate of the role of the inorganic chemist, who must partner with biologists, clinicians, physicists, pharmacologists, radiochemists and other specialists to move forward in this highly multidisciplinary field. The material is arranged roughly by periodic group,

with some flexibility in this approach to allow for parallels in applications to be grouped together where this is appropriate; lanthanides and actinides are accorded the status of “honorary groups” rather than periods for this purpose. Only elements that have radioisotopes with a significant current or promising clinical or research application are included; some groups offer greater riches in this respect than others. Elements of particularly current topical interest are considered in somewhat more detail.

Group 1

In group 1, only rubidium offers an imaging radioisotope with a significant biomedical application – the short half-life positron emitter ^{82}Rb (β^+ , 95%, half-life 75 s). As a group 1 metal whose chemical speciation under biological conditions is almost completely restricted to the hydrated cation, its potential for incorporation into complex targeting molecules is negligible. Nevertheless, its periodic position underlies its application; Rb^+ is a potassium mimic and its ionic radius, despite being larger than that of K^+ , does not prevent it serving as a substrate, in place of K^+ , for the Na^+/K^+ -ATPase, a ubiquitous antiporter in cell plasma membranes that pumps potassium ions into cells and sodium ions out, in the ratio 2:3, driven by and coupled to the hydrolysis of ATP. This pump is most abundant and active in the myocardium, resulting in $^{82}\text{Rb}^+$ that has been delivered to the heart via blood becoming trapped rapidly in the myocardium, provided blood flow is adequate to deliver it and the tissue is sufficiently metabolically active and energetic to drive the pump. Images of the distribution in the myocardium, obtained by PET, provide a map of its perfusion, giving valuable information about the patient’s condition for the cardiologist.¹ An example is shown in Fig. 2.

The excellent utility of this radioisotope for this purpose arises from its high-abundance positron emission, and its availability from a convenient generator in which the parent isotope is strontium-82 (half-life 25 days), adsorbed on a solid phase such as stannic oxide, decays to ^{82}Rb which is eluted with physiological saline. Because of the 75 s half-life, there is not time for manipulation with syringes or procedures for radiolabelling or sterilisation, and the generator is “plumbed” directly into the vein of the subject via an infusion set. The short half-life allows repeated administration and imaging after a short interval, while keeping the radiation dose to the patient low. Although costly, this is now a commonplace procedure especially in the US.

Myocardial perfusion scanning using the ^{82}Rb -generator relies on the same biochemical principle as the older (>30 years) use of monovalent thallium-201 (gamma-emitter), which is also a potassium mimic, for obtaining similar clinical diagnostic information with a gamma camera (see Group 13). $^{201}\text{Tl}^+$ scanning has also been applied in the past to tumour imaging, relying on the same biochemical pathway, suggesting that application of ^{82}Rb could be extended in the same way. Accordingly, a recent evaluation in patients with colorectal and lung cancer confirmed tumour avidity of the tracer and the ability to map tumour perfusion (Fig. 2),² opening up a new clinical field of application for this radionuclide.

Group 2

Like the group 1 elements, the group 2 metals are not amenable to kinetically stable incorporation into molecules and bioconjugates, and their radioisotopes find their application mainly through mimicry of calcium. Thus the beta emitter strontium-89 (half-life 53 days) has been used for many years as a palliative therapy for painful bone metastases in cancer, especially prostate cancer, by exploiting toxicity of the beta emissions, most likely towards inflammatory cells in these lesions. After intravenous administration of $^{89}\text{SrCl}_2$, the strontium is transported in way that, to an extent, mimics calcium and it accumulates in sites of active bone mineral deposition (rather than mineral lysis, as found in for example multiple myeloma bone lesions) found in such metastases, leading to higher radiation doses in these tumours than in normal tissues.³ ^{89}Sr has no positron or gamma emissions and so is not amenable to high quality quantitative imaging, but the positron emitter ^{83}Sr (β^+ , 24%, half-life 33 h) which is produced by proton irradiation of ^{85}Rb in a cyclotron,⁴ or the gamma emitter ^{85}Sr (γ , 100%, half-life 65 days) can in principle be used to determine its quantitative biodistribution.

The other group 2 radionuclide of major importance emerging recently is radium-223 (α , 94%, half life 11.4 days), an alpha emitter, which also mimics calcium in accumulating selectively in sites of bone mineralisation (Fig. 3). The recent success of clinical trials of $^{223}\text{RaCl}_2$ in patients with metastatic prostate cancer represents the first major application of alpha emitting isotopes in humans. It is a significant step forward in therapeutic nuclear medicine opening the door to wider use of alpha-emitter therapy in other cancers.

Applications of these therapeutic isotopes in other cancers will require their incorporation into more complex targeting molecules, which is extremely challenging for the group 2 metals as they do not readily form kinetically stable chelates; indeed, the development of novel chemistry to incorporate these metals into bioconjugates with a degree of kinetic stability might be considered a challenge to inorganic chemists. The insoluble nature of many of their salts, including minerals such as hydroxyapatite, may offer the possibility of incorporating them into inorganic nanoparticles. These could then be targeted by derivatising their surface using conjugates of targeting biomolecules with phosphonates and bisphosphonates, which form stable links with the surface of such nanoparticulate materials.

6

Group 3

While the basis of the uses of the group 1 and 2 elements is restricted to mimicry of the biological behaviour of their biologically important congeners (namely potassium and calcium), from group 3 onwards there is opportunity to incorporate the radioelement into more complex molecules and bioconjugates for targeted molecular imaging, by chelation or covalent bond formation. From a historical perspective the Group 3 elements are not an ideal starting point since the groundwork for their applications was laid in past decades using related trivalent metals from other parts of the periodic table, especially Group 13 and lanthanides (*vide infra*). The trivalent, “hard” metal ions from these groups find their main applications as radiolabels for biomolecules, incorporated with use of bifunctional chelators

(Fig. 4) which share, to an extent, common design features but with subtle variations to suit individual metals. These are discussed in more detail in their respective sections and have recently been much more comprehensively reviewed elsewhere.⁷

Group 3 is represented by scandium-44 (β^+ , 94%, half-life 3.97 h), yttrium-90 (β^- , 100%, half-life 64 h) and yttrium-86 (β^+ , 33%, half life 14.7 h). ^{44}Sc is a recent innovation,⁸ available through development of the $^{44}\text{Ti}/^{44}\text{Sc}$ generator and offering the possibility, after further development, of a PET radionuclide chemically similar to gallium-68 (*vide infra*) but for applications requiring a somewhat longer half-life (3.97 h c.f. 68 min). The ^{44}Ti parent has a long half-life of 60 years, which raises problems with radioactive waste management. There is potential for a “theranostic” (PET imaging/radionuclide therapy) pair by using it alongside the potential therapeutic radionuclide ^{47}Sc (β^- , 100%, half-life 3.35 days).⁹ DOTA-based chelators (**1**, Fig. 4) have been employed to link it to targeting biomolecules.

^{90}Y is a pure high-energy (2.28 MeV) beta-emitting radionuclide that has growing applications in radionuclide therapy when coupled to small tumour-targeting peptides and monoclonal antibodies. Its beta emissions have a relatively longer range - about a centimetre in tissue - compared to other therapeutic beta emitters such as ^{131}I and ^{177}Lu . Most prominent currently among the targeting molecules used are the somatostatin analogues, used for radionuclide therapy of neuroendocrine and other tumours that express somatostatin receptors,¹⁰ and the antibody-based treatment Zevalin for lymphoma.¹¹ The yttrium is coupled to the targeting peptide or antibody by means of a bifunctional chelator with amine and carboxylate donors, such as the macrocyclic DOTA and non-cyclic CHX-A''-diethylenetriaminepentaacetic acid (**2**), Fig. 4 (*vide infra*). Since ^{90}Y has no positron or gamma emissions, quantification of its biodistribution by imaging to assess radiation doses is difficult, and analogues labelled with the gamma-emitter indium-111 have been used as surrogates for this purpose. Inorganic chemists will recognise that this poses uncertainties because the coordination chemistry of indium and yttrium is subtly different and can (and does) lead to differences in biodistribution and clearance. Therefore to obtain definitive and quantitative biodistribution information to underpin radionuclide therapy, the positron emitting isotope ^{86}Y , which can be produced on many biomedical cyclotrons, can be used.¹²

Group 4

Zirconium-89 (β^+ , 23%, half-life 78.4 h) is a rising star in Group 4, emerging in response to the need for a longer half-life positron emitter to match the growth in availability of PET scanners in the last decade. ^{89}Zr is quickly becoming the PET replacement for the gamma-emitter indium-111 (see Group 13), which, with its half-life of 67.3 h, has been the radioisotope of choice since the 1980's for labelling molecules with slow pharmacokinetics, i.e. mainly monoclonal antibodies. IgG antibodies clear very slowly from blood and continue to accumulate in tumour targets and improve target-to-background ratios over a period of several days. Consequently a relatively long half-life is required, and imaging is typically carried out 24-72 h after injection of the tracer. The improvements in image sensitivity and quantification offered by PET compared to SPET have created a desire for a radionuclide with similar chemistry (i.e. amenability to kinetically stable chelation) and radiological half-life. Despite some disadvantages (low positron yield, abundant high-energy

gamma emissions, both of which lead to concerns about high patient radiation dose), ^{89}Zr fits this need. This presents a new challenge for inorganic chemists: new chelators are needed that impart both kinetic stability and efficient, mild labelling that overcomes the tendency towards hydrolysis in higher pH conditions, while fundamental studies of the coordination preferences of Zr^{4+} are less complete than is the case for some other metals described in this article. A number of bifunctional chelators conventionally used with the trivalent metals (see Group 13; Fig. 5), such as DOTA and DTPA derivatives were evaluated without great success but, somewhat fortuitously, the iron chelator desferrioxamine-B (DFO, **3**, Fig. 4) proved to combine the most efficient labelling with the best long-term *in vivo* stability, despite the general acceptance of DFO as a ligand for hard trivalent metals rather than tetravalent ones such as Zr^{4+} , and despite the fact that it cannot satisfy the evident preference shown by zirconium for coordination numbers greater than 6 (Fig. 5). $^{13}\text{Zr}^{4+}$ readily transchelates from the oxalate complex $[\text{Zr}(\text{oxalate})_4]^{4-}$ (the form in which it is most often purified from the yttrium target after proton irradiation in the cyclotron) to form the DFO complex under mild conditions. Antibodies labelled with ^{89}Zr through conjugation with DFO allow imaging for several days, in both experimental animals and humans, with very little loss of ^{89}Zr (which is manifested in uptake in the bones and joints, as exemplified in Fig. 6). This has made possible the use of ^{89}Zr -PET to evaluate the biodistribution in humans of several candidate antibody therapeutics,^{13–16} and to demonstrate the advantages of ^{89}Zr -PET over SPET (even with the optimal SPET isotope $^{99\text{m}}\text{Tc}$), for example in sentinel lymph node imaging in humans.¹⁷ Efforts are in progress to develop ligands with superior Zr^{4+} chelation properties compared to DFO, including the tripodal tris(hydroxypyridinone) hexadentate chelator YM10318 (**4**, Fig. 4) developed for use with gallium-68.¹⁹ A promising strategy is represented by octadentate designs based on a tetrapodal array of four bidentate oxygen donor ligands.^{20, 21} The structure of the Zr^{4+} tetrakis(*N*-methylacetohydroxamate) complex, which has a 4:1 ligand:metal stoichiometry forming a mononuclear eight-coordinate structure²² (Fig. 5), suggests that an assembly of four such bidentate ligands is the ideal way to meet the coordination preferences of zirconium. It has been most conveniently and elegantly implemented by linearly extending the DFO ligand to include a fourth hydroxamate group, producing an octadentate ligand **13** that on (very preliminary) evaluation appears to have the expected advantages over DFO itself²³ (Fig. 5). This is a highly topical endeavour in radiometal chemistry; nevertheless, it should be recognised that, meanwhile, DFO itself is an extremely effective chelator (Fig. 6), with only slight translocation of radioactivity from labelled antibody to bone allowing high-quality PET imaging to be continued clinically.

Another application, of growing importance, that calls for a long half-life positron emitter is radiolabelling of living cells for tracking their migration through the body over a period of several days. This has been a major role for the gamma-emitter ^{111}In (see Group 13) for more than three decades, but the advantages of PET over SPET stimulated a search for positron-emitting analogues. Despite the difference in preferred oxidation state, there are parallels in chemical behaviour that provide a rationale for design of such tracers. Thus, by analogy with the metastable lipophilic complex $[\text{InL}_3]$ (*L* = bidentate uninegative ligand such as oxinate and tropolonate, Fig. 7), which non-specifically diffuses into cells and dissociates allowing the released In^{3+} to bind to intracellular macromolecules, Zr^{4+} forms

metastable lipophilic complexes $[ZrL_4]$ which behave similarly. The ^{89}Zr oxinate complex has shown great promise in labelling a range of cell types, giving, in addition to the imaging advantages of ^{89}Zr over ^{111}In , equivalent cell labelling yields, better cellular retention of radioactivity and lower toxicity *in vivo* than ^{111}In . Cancer cell migration has been followed for up to 14 days in a mouse model of multiple myeloma using this tracer (Fig. 7).²⁴

Group 5

Very recently niobium-90 (β^+ , 53%, half-life 14.6 h) has emerged as a promising radionuclide for positron emission tomography (PET). To date, although it can be attached to monoclonal antibodies using the bifunctional chelator DFO, limitations in the separation chemistry have impeded attempts at exploring the radiochemistry and imaging potential.²⁵ Tantalum-178 (γ , half-life 9.3 min) is generated and concentrated on site as needed from W-178 (half-life 21.7 days) using a semi-automated generator system to maximise consistency.²⁶ Its chemistry has not been developed for specific targeting applications.

Group 6

Chromium-51 (γ , 9.9%, half-life 27.8 days) emits gamma rays of too high energy, and has too long a half life, for imaging applications but is used in nuclear medicine for non-imaging tracer applications. Molybdenum-99 and tungsten-188 are indirectly important as parent isotopes for technetium-99m and rhenium-188 (see Group 7).

Group 7

Manganese-52m (β^+ , 98.3%, half-life 21.1 min) can be produced from the $^{52}Fe/^{52m}Mn$ generator, and in unchelated form (most likely Mn^{2+}) is rapidly taken up in the myocardium and is a potential myocardial perfusion agent.²⁷ However, it has not been adopted in clinical use.

Technetium-99m (γ , 90%, half-life 6.02 h) has for several decades been the radioisotope used in the largest number of clinical radionuclide scans, and the invention of the ^{99m}Tc generator, enabling daily availability of radiopharmaceuticals in all major hospitals, was one of the key steps in the evolution of nuclear medicine as a routine service. The generator overcomes the problem of worldwide distribution of the short half-life (6 h) radionuclide, by enabling it to be shipped in the form of its parent radionuclide molybdenum-99 (half-life 60 h), as molybdate bound to an alumina stationary phase. Upon decay of ^{99}Mo , $[^{99m}Tc]$ -pertechnetate is formed and can be eluted from the stationary phase with physiological saline. The chemistry of technetium is so diverse, and its importance to nuclear medicine so great (because of the generator availability, because the single gamma photopeak at 141 KeV offers a close to ideal balance of attenuation and gamma camera sensitivity and resolution, and because many complexes can be synthesised by a simple one-step “kit” process) that it would warrant a Dalton Discussion to itself. Therefore, after a brief historical summary, this section will focus on the most current and topical developments.

Early implementation of ^{99m}Tc radiopharmaceuticals (1970s) was based on empirical biological evaluation of a variety of ^{99m}Tc chelates, with ligands such as dithiolates,

bisphosphonates and amino- and hydroxyl-carboxylates, without guidance from the detailed knowledge of technetium coordination chemistry that is available today. This led to the first generation of ^{99m}Tc radiopharmaceuticals, many of which are still in routine use today (e.g. ^{99m}Tc -MDP (**14**), ^{99m}Tc -DMSA (**15**, **16**), ^{99m}Tc -DTPA (**17**), ^{99m}Tc -HIDA (**18**), Fig. 8) for imaging bone disease, kidney perfusion, kidney function and liver function, respectively) despite lack of full understanding of their structure and mechanism. In the 1980s, a more design-and-mechanism based approach began to emerge, informed by a growing knowledge of the coordination and oxidation state preferences of technetium. This led to a range of technetium “cores” – stable metal complex units that could be modified to control pharmacokinetic and targeting properties, without loss of control of the technetium coordination sphere. This was the basis for the second generation of ^{99m}Tc tracers which include well-defined compounds such as lipophilic cations for myocardial perfusion imaging (^{99m}Tc -sestamibi, ^{99m}Tc -tetrofosmin)²⁸ and uncharged metastable lipophilic complexes capable of crossing the blood-brain barrier and cell-labelling (^{99m}Tc -HMPAO,²⁹ ^{99m}Tc -NOET³¹). In these, the biological behaviour is a consequence of the physicochemical properties of the complex such as charge, protic equilibria, lipophilicity, size, kinetic stability and reactivity, and possible redox reactivity. The development of a set of technetium cores³² including TcO^{3+} (e.g. **19**),³³ 34 TcN^{2+} (e.g. **20**),³⁵ $\text{Tc}(\text{CO})_3^{3+}$ (e.g. **21**),³⁶ 37 $\text{Tc}(\text{CNR})_6^+$ (e.g. **22**),³⁸ $\text{Tc}(\text{hynic})^{3+}$ (e.g. **23**),³⁹ etc., see Fig. 9) with well-defined coordination chemistry also laid the foundation for the incorporation of ^{99m}Tc into bioconjugates such as peptides and antibodies, and conjugates with small molecules and nanoparticles. Most current work is based on these established cores – there is rather little recent literature reporting new cores; one interesting recent example is the $\text{Tc}(\text{VII})$ core TcO_3^+ (e.g. **24**), to which the 3+1 cycloaddition of alkenes offers a potential new route to bioconjugation of ^{99m}Tc ⁴⁰, ⁴¹ (Fig. 8).

Despite the historical importance of ^{99m}Tc to nuclear medicine, the nuclear medicine community is approaching something of a crossroads in the development of technetium chemistry, and decisions will have to be made about how to, and indeed whether to, make its future secure. The world's supply of the parent isotope ^{99}Mo emanates from a small number of aging nuclear reactors, some of which have recently closed temporarily for planned refurbishment or unplanned repairs, during which ^{99m}Tc was in short supply and nuclear medicine departments resorted to alternatives (such as ^{201}Tl -TlCl for myocardial perfusion imaging (see Group 13) and ^{18}F -fluoride for bone metastases. This situation will inevitably repeat itself and the future unlimited availability of ^{99m}Tc cannot be assured without new investment – either in new reactors to produce more ^{99}Mo , or in development of alternative methods (e.g. cyclotron methods) to produce ^{99}Mo , or cyclotron routes to produce ^{99m}Tc directly.⁴² Given that the overriding advantage of ^{99m}Tc as the most widely used radioisotope in nuclear medicine is the $^{99}\text{Mo}/^{99m}\text{Tc}$ generator, cyclotron production of ^{99m}Tc has limited appeal because of distribution problems. At a time when PET is rapidly growing and the gallium-68 generator is set to make PET more widely accessible (see Group 13), perhaps even (to stretch a point) allowing ^{68}Ga PET to supplant ^{99m}Tc SPET as the workhorse of nuclear medicine, there are some hard decisions to be made in the near future.

Despite the present uncertainty, there is some innovation in $^{99\text{m}}\text{Tc}$ chemistry currently taking place. The main current challenges being addressed are improving the efficiency of bioconjugate labelling and the quality (homogeneity, specific activity, *in vivo* stability, target affinity) of the labelled product, and producing radiotracers for combined modality imaging (e.g. SPET/MRI, SPET/optical) for use with the emerging generation of combined modality scanners. One of the key attributes of $^{99\text{m}}\text{Tc}$ that has led to its predominance is the ability to synthesise a range of complexes in a one-pot, one-step process whereby [$^{99\text{m}}\text{Tc}$]-pertechnetate in saline (generator eluate) is simply added to a “kit” vial containing the necessary reducing agent, ligand and other constituents required to produce the desired radiopharmaceutical without need for purification or other subsequent processing. This simplicity means that many sterile $^{99\text{m}}\text{Tc}$ radiopharmaceuticals can be produced daily with minimal technologist input or costly equipment. While this is well-established for the “first generation” radiopharmaceuticals referred to above, the development of targeted $^{99\text{m}}\text{Tc}$ bioconjugates has not yet reached this level of simplicity. Until it does, these “third generation” $^{99\text{m}}\text{Tc}$ -labelled biomolecular imaging agents will not be routinely available to maximally benefit patients. The current most popular cores for bioconjugate labelling include $\text{Tc}(\text{hynic})^{3+}$, TcO^{3+} , and $\text{Tc}(\text{CO})_3^+$. All have limitations at present. Hynic is a bifunctional chelator that provides reasonably stable links to biomolecules, very efficiently at very low concentration, via one-step labelling, with high specific activity, at room temperature. However, while its coordination chemistry is better understood than when first introduced,^{39, 43} it is subject to exchange of co-ligands giving rise to mixtures of subtly different bioconjugates and potential co-ligand exchange *in vivo*. The ideal accompanying ligand to remedy these limitations (replacing tricine, ethylenediamine diacetic acid, water-soluble phosphines etc.) has yet to be introduced. The TcO^{3+} core can be linked to biomolecules by a variety of nitrogen- and sulfur-donor polydentate ligands such as mercaptoacetyl triglycine (MAG3, **19**),⁴⁴ 1,4,8,11-tetraaminododecane (**25**),^{45, 46} dimercaptosuccinic acid (**15**)⁴⁷ etc. (Fig. 8). These are highly stable but none have been developed into a simple, mild one-step labelling process. The $\text{Tc}(\text{I})$ tricarbonyl core $\text{Tc}(\text{CO})_3^+$ has been the subject of much attention and application, for labelling a range of small molecules, peptides and especially for radiolabelling proteins incorporating a histidine tag (a sequence of histidines first developed as a motif to assist protein purification during biological production). The labelling procedure requires first the synthesis of the putative intermediate [$^{99\text{m}}\text{Tc}(\text{CO})_3(\text{H}_2\text{O})_3$]⁺,³⁷ which is then incubated with the His-tagged protein producing a highly stable conjugate in which the technetium is coordinated by at least two imidazole groups of histidine residues. Recently, attempts have been made to place this bioconjugation step on a more efficient footing, by modifying the design of the His-tag, either to improve the biodistribution properties of the labelled protein^{48, 49} or to improve the labelling efficiency^{50–53} so that milder conditions can be employed and lower protein quantities can be labelled without need for the purification step (usually size-exclusion chromatography) which is usually a part of the process (Fig. 9). Incorporation of positively charged residues, and/or methionine or cysteine, adjacent to the His-tag sequence resulted in almost an order of magnitude increase in labelling efficiency when conjugating in phosphate buffers, for reasons that are yet to be elucidated.⁵³ This shows that there are ways in which the properties and general utility of biomolecule labelling with $^{99\text{m}}\text{Tc}$ can be improved, and

the further development of such methods to achieve a truly single-step, kit-based radiolabelling method for biomolecules is still a challenge for chemists.

The Tc(V) nitride core,³⁵ with the nitride ligand derived from hydrazine derivatives such as succinic dihydrazide, has recently been the subject of increased interest as a centre to which small molecules can be attached by means of dithiocarbamate ligands, a wide range of which can be easily synthesised by treatment of a primary or, preferably, secondary amine-containing molecule with carbon disulfide. This was first applied in the myocardial imaging agent ^{99m}Tc-NOET,^{54, 55} and more recently extended to other derivatives such as antibiotics, bisphosphonates and other drug-like molecules.⁵⁶ In some circumstances the presence of two dithiocarbamate ligands offers, in theory, the opportunity to improve target affinity. An attempt to exploit this to develop improved agents for imaging bone disease and small soft-tissue calcifications produced a bis(bisphosphonate) derivative (Fig. 10) with two pendant bisphosphonate groups) which shows higher *in vivo* stability than ^{99m}Tc-MDP and is able to image vascular calcification in small animal models. However, the extent to which it can improve on molecules containing just one pendant bisphosphonate group (such as the tricarbonyl derivative, Fig. 11), or even ^{99m}Tc-MDP, is as yet unproven. New synthetic precursors from which the nitride-ligand may derived have been developed recently, for both technetium and rhenium.⁵⁷

The arrival of combined modality imaging incorporating radionuclide and magnetic resonance contrast, to exploit simultaneously the advantages of each, has created interest in developing contrast agents that support both modalities in a single species. An attractive clinical use is sentinel lymph node imaging, where surgeons value both pre-surgical imaging (SPET to identify a location and MRI to provide soft tissue contrast and fine structural detail) to identify lymph nodes draining tumours prior to surgery, and fluorescent contrast as a guide during surgery (Fig. 11). Several versions of iron oxide nanoparticles derivatised with radionuclides for such purposes have been reported, including materials with ^{99m}Tc linked to the nanoparticle using the tricarbonyl core directly^{58, 59} or via a bisphosphonate linker⁶⁰ (Fig. 11); the latter provides greatly improved stability compared to the conventional carboxylate linker used to anchor various modifiers to the surface of iron oxides.

Beta-emitting isotopes rhenium-186 (β^- , 92.5%, half-life 90 h) and rhenium-188 (β^- , 100%, half-life 17 h) have been of interest to researchers for many years as therapeutic analogues of ^{99m}Tc radiopharmaceuticals. However, while other beta emitters such as yttrium-90 and lutetium-177 have become established in clinical use, so far rhenium isotopes have not made their presence felt widely in the clinic despite the convenience of the ¹⁸⁸W/¹⁸⁸Re generator, which is chemically analogous to the ^{99m}Tc generator. The chemical analogy between rhenium and technetium, which is often the basis of a diagnostic/therapeutic “matched pair” plan, must be implemented with caution⁶¹ since, when the ligand and core choice is not optimal to create thermodynamically and kinetically stable complexes with strongly preferred geometry and oxidation state, the structures, reactivity and biological behaviour may differ. The bisphosphonate complexes of technetium and rhenium, for example, behave very differently.⁶² On the other hand the tricarbonyl complexes, M(V) nitride-dithiocarbamate complexes and M(V) oxo-complexes (including those of MAG3, DMSA⁶³

and tetraamines), are closely similar in structure and reactivity when $M = \text{Tc}$ or Re , although they may require different synthesis conditions. The tricarbonyl core, in particular provides a highly stable and reliable means of synthesising structurally analogous protein and peptide conjugates⁶⁴ via the His-tag coordination chemistry described above for $^{99\text{m}}\text{Tc}$, and indeed the improvements in labelling efficiency shown in Fig. 9 apply equally to ^{188}Re . There is thus every prospect that high quality ^{188}Re radiopharmaceuticals could be developed for routine therapeutic use to exploit the convenience and potential cost-effectiveness of the ^{188}Re -generator, if an appropriate business model can be identified.

Group 8

Iron-52 is a positron emitter (β^+ , 55.5%, half-life 8.28 h) but has no advantages for general clinical use and is of interest mainly as a tracer for investigating iron metabolism and distribution in health and disease *in vivo*.^{65, 66} Even this application is complicated by the fact that its decay leads to manganese-52m, which is also a positron emitter (β^+ , 98.3%, half-life 21.1 min) so it is not possible to know that PET images reflect iron distribution rather than the redistribution of the decay product $^{52\text{m}}\text{Mn}$. This decay scheme can however be used as the basis of a generator system for producing the short half-life $^{52\text{m}}\text{Mn}$ ²⁷ (see Group 7).

Ruthenium-97 has attractive gamma emission properties (γ , 85%, half-life 2.9 days) that would make it suitable as a radiolabel for biomolecules with slow pharmacokinetics (i.e. applications similar to indium-111, see Group 13) but its production demands very high energy proton bombardment, limiting its availability and preventing general clinical development.⁶⁷

Group 9

Cobalt-55 (β^+ , 76%, half-life 17.5 h), as unchelated Co^{2+} , is believed to mimic transport of calcium ions and has found applications in imaging tissue damage especially in brain, e.g. in stroke and vascular dementia.⁶⁸ Its long half-life allows time for radiosynthesis to incorporate the isotope into structurally diverse targeting molecules, but this has been barely exploited.⁶⁹ Efforts to label cells for *in vivo* cell tracking have been largely unsuccessful.⁷⁰

Rhodium-105 (β^- , 100%, half-life 1.47 days) is a beta-emitter with potential applications in radionuclide therapy. Various bifunctional chelator systems based on combinations of soft donor groups (amine, thioether and phosphine) have been evaluated with some promise but have not yet translated into therapeutic evaluation.^{71–73}

Group 10

Nickel-57 (β^+ , 43.4%, half-life 35.6 h) has been briefly explored as a PET imaging radiolabel but its use has been limited to labelling of metal chelating drugs (doxorubicin)⁷⁴ and use in studying the toxicology of nickel itself.⁷⁵

Platinum-195m (γ , half-life 4 days) is a reactor-produced radionuclide that emits low-abundance gamma photons. It has been used primarily for studying the biodistribution and

pharmacokinetics of platinum anticancer drugs,⁵⁹ and also experimentally as a radionuclide therapy by virtue of its Auger electron emissions.⁷⁶

Group 11

Copper radioisotopes have made a major impact in the last two decades due to a combination of a versatile range of radionuclides for both imaging and therapy (Table 1), and chemical properties that are amenable to various imaging applications.^{77, 78} These properties include the kinetic stability of well-designed macrocyclic chelates,^{79, 80} suitable for labelling peptides and antibodies; well-defined redox properties, especially bioreduction from Cu(II) to Cu(I), that lead to applications in blood flow and hypoxia imaging;^{81, 82} and studies of the innate biological handling of copper and abnormalities in these processes associated with disease.⁸³ A range of isotopes for PET imaging is available, with half-lives ranging from 9 minutes (⁶²Cu, generator-produced) to 12.7 h (⁶⁴Cu, cyclotron-produced). In addition, ⁶⁴Cu (which is a beta- and Auger electron-emitter as well as a positron emitter) and ⁶⁷Cu (which combines beta and imageable gamma emissions) are attractive as therapeutic radionuclides. Despite early promise in clinical trials with ⁶⁷Cu-labelled antibodies, therapeutic application of ⁶⁷Cu has not lived up to expectations because of lack of a reliable and cost-effective production route, which remains unresolved.

Because of the attractive applications of the longer half-life isotopes ⁶⁴Cu (PET imaging and radionuclide therapy) and ⁶⁷Cu (radionuclide therapy and gamma imaging), many studies over the years have been devoted to identifying the best chelators for copper; some of the more significant ones are shown in Fig. 4; some more specific to copper are shown in Fig. 12. Early studies favoured macrocyclic ligands TETA (Fig. 12) and cyclam,⁷⁷ but with more experience DOTA, and most recently NOTA (**5**, Fig. 4) and the sarcophagine bicyclic structures^{84–86} (Fig. 12) have emerged as the leading chelators combining both high *in vivo* kinetic stability and high labelling efficiency at low chelator-antibody conjugate concentration under mild conditions.⁸⁷ Non-macrocyclic ligands are consistently inferior, and cross-bridged cyclams (Fig. 12) other than the sarcophagines, designed to impart kinetic stability by virtue of the greater rigidity imparted by the cross-bridge, are still being evaluated.^{88, 89} In general, cross-bridging leads to greater kinetic stability, but also to a higher activation energy barrier to complex formation, leading to slower labelling and a requirement for harsher conditions. The sarcophagine ligands appear to represent an appropriate balance between these two effects. Despite the effective labelling and good stability in blood shown by antibodies labelled with ⁶⁴Cu via NOTA and DOTA derivatives, a comparison of peptides labelled with ⁶⁴Cu, ⁶⁸Ga and ¹¹¹In via these ligands suggested that dissociation of copper from the chelator, once the conjugate enters cells, leads to translocation of ⁶⁴Cu to liver and hence to gut. This does not occur for the ¹¹¹In and ⁶⁸Ga labelled conjugates, indicating that these ligands remain far from optimal for tracking biomolecules with ⁶⁴Cu.⁹⁰ The design of bifunctional chelators for copper remains a highly active area.

The redox properties of copper can be exploited in several different ways and for different purposes in diagnostic imaging. The common putative mechanistic theme in all these applications is that lipophilic Cu(II) complexes of bis(thiosemicarbazone) ligands (Fig. 13)

diffuse into cells non-specifically, whereupon they are exposed to intracellular reducing agents causing reduction to Cu(I). The complexes may then dissociate either slowly (in the case of ATSM and related complexes with two backbone alkyl groups) or quickly (PTSM, GTSM and other complexes with <2 backbone alkyl groups). Once liberated from the ligand, the copper becomes subject to the cellular processes involved in tight regulation of intracellular copper, leading to incorporation into proteins or efflux from the cell, depending on the cell type. The slowly-dissociating complexes can be re-oxidised by molecular oxygen in the cell, whereupon they may escape by diffusing out, as the concentration gradient that drove them in is reversed by clearance from blood and excretion. This is the hypothetical basis of selectivity for hypoxic cells in CuATSM and related complexes,^{91–94} although other factors also appear to control the cellular uptake and *in vivo* biodistribution of copper administered in the form of CuATSM.^{95–98} The rapidly-dissociating complexes, on the other hand, show no selectivity and deposit copper in cells and tissues in proportion to their delivery via blood, hence they are effectively blood flow imaging agents.

This non-specific trapping has been put to use in cell labelling with ⁶⁴CuPTSM⁹⁹, ⁶⁴CuGTSM¹⁰⁰ and ⁶⁴CuGTSM, both of which show extremely efficient uptake and initial trapping in cells.¹⁰¹ Lipophilic ⁶⁴Cu(dithiocarbamate) complexes behave similarly.¹⁰¹ However, cell tracking over the period of days allowed by the half-life of ⁶⁴Cu is not effective because the copper-regulating processes cause efflux of copper over a period of several hours.¹⁰¹ To an extent this problem might be overcome by prior treatment of cells with chelating agents that will sequester ⁶⁴Cu released inside the cell, preventing their transport out by specific cellular transport mechanisms.¹⁰² This approach deserves further evaluation, since cell tracking with ⁶⁴Cu is an attractive application because of the high-resolution PET imaging achievable with ⁶⁴Cu.

Non-specific trapping of CuPTSM and particularly CuGTSM is also being used as a basis for imaging biological transport processes for copper. Thus, ⁶⁴CuGTSM can efficiently deliver ⁶⁴Cu across the blood brain barrier and release it into cells (in contrast to, for example, CuATS which does not cross the blood brain barrier¹⁰³). The resulting intracellular deposition of copper is sufficient to monitor the fate of the copper as it is exported from cells and redistributed; ionic ⁶⁴Cu (e.g. Cu(acetate)₂), on the other hand, does not enter cells and tissues in sufficient quantities for this to be possible, and uptake in tissues reflects entry of copper into cells via specific transport systems. Thus, both delivery/influx and efflux mechanisms can be imaged separately. This can be applied to imaging changes (and early indications indicate that there are indeed imageable changes) in copper homeostasis and transport associated with disease, including Alzheimer's disease¹⁰⁴, ¹⁰⁵ and other dementias, Menkes' disease, and Wilson's disease,⁸³ and their treatment with copper-chelating drugs. Recent observations of uptake of ⁶⁴Cu administered as ionic copper in tumours, including changes in uptake due to hypoxia, indicate that there are some interesting applications of tracking copper metabolism in tumours as well.⁹⁵, ¹⁰⁶ The full potential for imaging changes in copper metabolism to diagnose disease is only just beginning to dawn, and this represents a big opportunity and challenge for metals in imaging over the next few years.

Hypoxia imaging with CuATSM is an important application, as hypoxia is a prognostic factor for response of tumours to radiotherapy and there are many other clinical indications for hypoxia measurement. It has been a subject of controversy recently because of observations that ionic ^{64}Cu shows a biodistribution that is similar to that of $^{64}\text{CuATSM}$, including in some tumours studied.⁹⁵ This is compounded by the likely mechanism, which entails dissociation and hence rapid release of free copper, resulting in potential supposition that ^{64}Cu distribution after administration of $^{64}\text{CuATSM}$ reflects distribution of ionic copper rather than hypoxia, and that in some tumours uptake of ionic copper may be related to hypoxia as well. These questions certainly complicate the interpretation of the $^{64}\text{CuATSM}$ scans. However, Cu bis(thiosemicarbazone) complexes do not behave like unchelated copper in the early phase of biodistribution; CuATSM is hypoxia-selective, CuPTSM is (almost) not;^{92, 107} CuGTSM is taken up in normal myocardium, CuATSM is not;¹⁰⁵ CuATSM and CuGTSM cross the blood brain barrier, CuATS and ionic copper do not.¹⁰³ These differences are evident from Fig. 13. The most likely underlying mechanism is that all the complexes are, to a large extent, quickly metabolised in liver, releasing copper, part of which is excreted into the gut via the bile, and part of which is recirculated as copper transport proteins, leading to delayed uptake in tissues by specific copper transport mechanisms, which may themselves be disturbed in tumours and in hypoxic tissues. Since the clearance of CuATSM from non-hypoxic tissues is relatively quick, imaging can be performed early (e.g. 20 min), as in most studies in Japan (where the short lived isotope ^{62}Cu is most often used). New, less lipophilic analogues of CuATSM (e.g. CuATS and CuCTS, Fig. 13) show promise as potential superior replacements for CuATSM; they clear more quickly from normoxic tissue and reach higher hypoxic:normoxic tissue ratios in isolated rat hearts in a shorter time.¹⁰⁷ *In vivo* evaluation of these compounds is anticipated with interest.

Much of the clinical work with CuATSM, especially in Japan, has been done with ^{62}Cu . A ^{62}Cu generator is not commercially available in Europe and very little work with ^{62}Cu has been reported outside Japan.¹⁰⁸ For clinical trials its short half-life (9 min) has the advantage of offering the opportunity to perform repeat scans with and without an intervention (e.g. oxygen breathing), with the patient in the same position on the scanner. For such purposes a $^{62}\text{Zn}/^{62}\text{Cu}$ generator has been implemented at King's College London by means of a collaboration in which natural copper is irradiated using the cyclotron at the University of Birmingham, and the resulting ^{62}Zn is processed to fabricate the generator at King's. Fast chemistry for synthesis of $^{62}\text{CuATSM}$ (to GMP standards) and other bis(thiosemicarbazone) complexes has been developed by implementing the solid phase transmetallation method reported by Dilworth et al.¹⁰⁹ whereby the ligand, in the form of a zinc complex, is linked to a solid phase via a pyridine ligand, which binds an axial site of zinc. Passage of ^{62}Cu solution over this stationary phase allows transmetallation to form the copper complex, releasing the ligand from the column and providing a product very quickly and with very high specific activity. This opens the door to several interesting clinical trials with very low radiation doses to patients.

Because of its half-life, availability and excellent PET imaging properties, ^{64}Cu has been a radioisotope of choice in radiolabelling nanoparticulate materials^{110–112} to assess drug delivery and combine imaging modalities. An example of the latter is radiolabelling of magnetic iron oxide nanoparticulate contrast agents with ^{64}Cu using the

bis(dithiocarbamate-bisphosphonate) complex shown in Fig. 14, in which the bisphosphonate groups anchor the ^{64}Cu to the inorganic particle surface, allowing the potential of the new generation of PET/MRI scanners to be applied, for example, to sentinel lymph node localisation.¹¹³

Other Group 11 metallic isotopes of interest to molecular targeting include ^{111}Ag ¹¹⁴ and ^{198}Au ¹¹⁵ (beta-emitters with potential, if not yet actual, application in targeted radionuclide therapy).

Group 12

^{62}Zn is important as the parent isotope in the $^{62}\text{Zn}/^{62}\text{Cu}$ generator (see Group 11). ^{197}Hg -chlormerodrin¹¹⁶ (γ , 100%, half-life 64.14 h) was used in the early days of nuclear medicine as a renal perfusion agent before replacement with $^{99\text{m}}\text{Tc}$ tracers. ^{197}Hg can be coupled to biomolecules using a bifunctional chelator incorporating the soft macrocyclic ligand 1,4,7-trithiacyclonane.¹¹⁷

Group 13

Group 13 is a feast for the radiometal molecular imager. Gallium, indium and thallium have radionuclides of great historic and current importance, and even boron and aluminium, while offering no useful radionuclides, have come to prominence very recently because of their role as inorganic binding sites for the important radionuclide fluorine-18, a role which will be discussed under Group 17.

Gallium-67 (γ , 86%, half-life 3.26 days) has been important in nuclear medicine for decades. Among the various applications and complexes explored are two main clinical roles: imaging of lymphoma and other tumours,^{118, 119} and imaging of infection.¹²⁰ Uptake in lymphoma is believed to be mediated by transferrin receptors, taking advantage of the serum speciation of gallium when administered as the citrate complex, which involves a significant fraction of the radionuclide binding to the iron-binding sites of the iron transport protein transferrin (reliable experimental evidence for this mechanism, however, is hard to pin down in the literature).¹²¹ The clearance of radioactivity from blood is very slow, resulting in delays of several days before useful imaging can be performed, making the long half-life of ^{67}Ga essential to this application. The mechanism by which ^{67}Ga (again administered as citrate complex) is accumulated in sites of infection is unclear and may be related either to targeting of the infiltrating immune cells, or targeting the microorganisms themselves, by binding to secreted polysaccharides or by transchelation to bacterial siderophores followed by siderophore-mediated uptake into the bacterial (or fungal) cells. Thus, these applications might rely fundamentally on the biological mimicry of iron by gallium.

A newly-emerging potential role for ^{67}Ga arises from the Auger electron emissions that accompany its nuclear decay, offering possible application as a therapeutic radionuclide. These electrons are higher in number and energy than some other Auger electron emitters, leading to substantial local radiation dose to the individual cells in which the ^{67}Ga is located. The higher energy means that the radionuclide may not need to be located within the cell

nucleus in order to have DNA damaging effects. Early indications supported the idea that ^{67}Ga may be more cytotoxic than ^{111}In which has previously been evaluated as a radionuclide therapy agent in clinical trials.^{122–127} The radiobiological effects of intracellular ^{67}Ga on cell survival warrant further study, in light of recent improvements in chelation and delivery of gallium isotopes.

^{68}Ga (β^+ , 88.9%, half-life 68 min) is set to make an impact on PET imaging comparable to that made by $^{99\text{m}}\text{Tc}$ half a century ago. It is a generator produced positron-emitting isotope with a half-life of 68 min – long enough for reasonably quick radiolabelling chemistry and for biodistribution of most small molecules, peptides etc., but short enough to keep radiation doses reasonably low. Despite commercial generators with marketing authorisation not having been available, many centres, especially in Europe, have been using ^{68}Ga clinically, mainly in the context of somatostatin receptor-targeting peptides such as DOTATATE, DOTATOC and analogues,^{128, 129} to which the radiometal is attached via a DOTA chelator (Fig. 4). Many of the technical issues that have delayed the regulatory approval of the generator have now been overcome and in 2014, the first marketing authorisation for a $^{68}\text{Ge}/^{68}\text{Ga}$ generator was granted by the EMEA and clinical use of ^{68}Ga is likely to spread and increase greatly, creating a second revolution in clinical PET (the first being the spread of cyclotrons and PET scanners driven by the enormous clinical utility of ^{18}F -fluorodeoxyglucose) by making it available in centres that do not have a cyclotron nearby. One might provoke a lively discussion by observing that this development coincides with the current (and probably future) era of shortages of $^{99\text{m}}\text{Tc}$, and could be a factor that informs decisions about the future of $^{99\text{m}}\text{Tc}$ as the workhorse of nuclear medicine (see Group 7). The arrival of the generator has sparked a proliferation of new ^{68}Ga imaging agents, particularly biomolecules such as peptides and small proteins, and conjugates of small molecules such as bisphosphonates^{130, 131} and folic acid,^{132, 133} to make economic use of the generator to bring its benefits to the maximum number of patients world wide. The development of new agents, and in particular their widespread application, requires radiolabelling chemistry that can be performed quickly, with the minimum of manipulation and the minimum of costly equipment, on the hospital premises. That is, labelling methodology akin to the $^{99\text{m}}\text{Tc}$ labelling kits that made radiopharmaceuticals available at low cost, that can be performed in facilities little more complex than conventional hospital radiopharmacies rather than PET radiochemistry centres with cyclotrons and arrays of robotic synthesisers and hot cells.

Despite having become the standard bifunctional chelator used in the first wave of ^{68}Ga -labelled peptides, DOTA (Fig. 4) was not designed specifically for Ga^{3+} chelation and is not ideal because labelling it requires relatively harsh conditions – heat (e.g. 90°C), time (30 min) and low pH, all of which bring inconvenience and undesirable complexity and may be incompatible with the biomolecule concerned. The last few years has seen something of a “beauty pageant” of new bifunctional chelators for ^{68}Ga , aiming to improve the labelling conditions and efficiency while maintaining adequate *in vivo* stability. A selection is shown in Fig. 4; a more comprehensive selection is discussed in an excellent recent review of metal chelators for radionuclides.^{7, 134} Many of these ligands, such as HBED (**6**, Fig. 4), DEDPA (**7**) and TRAP (**8**), significantly improve the labelling conditions compared to DOTA, and have good biostability and other potential advantages. Indeed HBED is the basis of very

promising ^{68}Ga -bioconjugates (e.g. the PSMA ligand for imaging prostate cancer) now being used in the clinic.¹³⁵ For rapid labelling under the mildest conditions at the lowest concentrations, the acyclic tripodal tris(hydroxypyridinone) ligand CP256, and its bifunctional conjugate YM103 (4, Fig. 4), appear to be the optimal choice, based on direct side-by-side comparison with some of the other ligands. Its design was based on the premise that rapid, mild and efficient labelling overrides *in vivo* stability as an important feature, because of the short half-life. The immediate future promises rapid development in this field and a small number of purpose-designed gallium chelators will soon emerge as a basis for commercial development of kit-based ^{68}Ga labelled radiopharmaceuticals.

A surprising property of YM103 is its ability to transchelate ^{68}Ga bound to transferrin in serum. This has been demonstrated *in vitro* by incubating in serum.¹⁹ The extent to which other chelators can do this has not been established but it raises the intriguing possibility of radiolabelling *in vivo*. This has been demonstrated by injecting ^{68}Ga acetate into mice, observing the typical slow clearance from blood to bone, and following with an injection of CP256 whereupon the circulating ^{68}Ga is immediately cleared from the circulation and excreted via the kidney (Fig. 15). Such behaviour, on a longer timescale, has been demonstrated previously for DFO using ^{67}Ga .^{136, 137} This *in vivo* transchelation is being explored as a basis for pretargeting with antibodies: injection of an antibody-YM103 conjugate, followed after a suitable period to allow targeting by an injection of ^{68}Ga -acetate. The pre-injected antibody perturbed the biodistribution of the ^{68}Ga , increasing its uptake in the tissues targeted by the antibody. This observation indicates potential for a new form of pre-targeting based on *in vivo* metal transchelation,¹³⁸ allowing use of short half-life radioisotopes such as ^{68}Ga even with targeting biomolecules that have very slow pharmacokinetics.

The similarity in ligand donor and geometric preferences between Ga(III) and Fe(III) underlies a new application of molecular imaging that is specific to gallium: species-specific imaging of microbial infection (bacterial or fungal) using ^{68}Ga -labelled siderophores. This exploits the microorganisms' highly developed systems for acquiring iron from their environment, in which they secrete low molecular weight chelators (siderophores) which bind Fe(III) with extremely high affinity, and then take up the complexes via specific transporters. By labelling these molecules with ^{68}Ga in place of iron, the structural analogy of the complex is adequate for the Ga complex to be taken up by the siderophore receptor, allowing this molecular mechanism to be used for specific imaging of the presence of the living microorganisms *in vivo*. This has been applied to detect *Aspergillus fumigatus* infection using its specific siderophores desferri-triacetylfusarinine C (TAFC) and desferri-ferricrocin (FC) (Fig. 16), and similarly other microbe/siderophore combinations, in animal models.^{139–142} This represents a highly promising new area for development.

Indium-111 (γ , 100%, half-life 2.8 days) was the first radionuclide to be commercially and clinically established in routine practice in gamma imaging applications that necessitate a long half-life: labelling monoclonal antibodies and labelling cells. Its commercial development in the 1980's coincided with the emergence of monoclonal antibody technology, which underpinned hopes of "magic bullet" drugs and diagnostics. It forms reasonably stable chelates with various polyaminocarboxylates and unlike copper it does not

appear to be essential to use a macrocyclic chelator for ^{111}In . Even the prototype DTPA (9, Fig. 4), coupled to antibodies by reaction of its cyclic anhydride with amine side chains of lysine residues, provided excellent results in the early days of antibody imaging, and was the chelator employed in the first commercially available peptide-based imaging agent Octreoscan.¹⁴³ DTPA has since been supplanted by related ligands (Fig. 4) offering greater kinetic inertness through incorporation of cross-bridging, backbone alkylation and cyclisation, e.g. DOTA¹⁴⁴ or CHX-A''-DTPA¹⁴⁵. ^{111}In remains the most important gamma-emitting radiolabel for antibodies (see for example Fig. 17).

Cell labelling with ^{111}In , developed to allow clinical imaging and localisation of infection and inflammation sites, was first developed in the late 1970s and entered widespread clinical use in the 1980s. The design principle was the opposite of that required in antibody labelling – rather than kinetic stability the aim was to form biologically unstable lipophilic complexes able to diffuse into cells and dissociate when exposed to the intracellular milieu. This was achieved with a number of uninegative bidentate ligands such as oxinate and tropolonate, forming InL_3 complexes (Fig. 7) and these complexes remain in demand for imaging inflammation and infection.¹⁴⁶ The rise of cellular therapies (transplants, stem cells etc.) has created new applications for cell tracking and ^{111}In is likely to continue to fill this need for some time to come.

Thallium-201 (γ , 10%, half-life 73 h), in the form of thallium(I) chloride, was the first routinely used myocardial perfusion imaging agent. Since it became established in clinical use it has become recognised that the $^{201}\text{Tl}^+$ cation, like rubidium discussed earlier, is a potassium mimic and a substrate of the sodium/potassium ATPase and so, like $^{82}\text{Rb}^+$, is efficiently taken up in well-perfused myocardium.¹⁴⁷ Despite its low γ -yield (which is compensated by a higher abundance of X-ray emissions) it remained the regular clinical myocardial imaging agent until supplanted by the lipophilic cationic technetium complexes, and made something of a come-back during recent $^{99\text{m}}\text{Tc}$ shortages. Its cationic charge was, misguidedly but ultimately successfully, the design template¹⁴⁸ for these hugely commercially successful new $^{99\text{m}}\text{Tc}$ myocardial agents developed in the 1980s; these are in fact not potassium mimics but are trapped in mitochondria by virtue of their cationic charge, and access them by virtue of their lipophilicity.¹⁴⁹ ^{201}Tl has been (and is in many centres) also used to detect tumours, being taken up presumably by the same mechanism.

Group 14

Group 14 offers carbon-11 (β^+ , 99.6%, half-life 20 min). This radioisotope makes possible the labelling of organic compounds without structural modification and provides a role for synthetic organic chemists in molecular imaging, which is outside the scope of this Perspective. In this field there is no escaping the dependence on a local cyclotron, automated multi-step synthesis and purification and so the challenges are rather different to those of inorganic radiochemistry. Other contributions from Group 14 include tin-117m (γ , 86%, and conversion electron emitter, half-life 13.6 days) which, as its Sn(IV) DTPA complex, shows exquisite selectivity for bone metastases, where its very short range electron emissions keep bone normal marrow irradiation to a minimum.¹⁵⁰ Despite this advantage it has not become established as a widely-used bone therapy agent, possibly because of limitations on the scale

of production. Lead-212 (β^- , 100%, half-life 10.6 h) is of interest as an “*in vivo* generator” of the alpha-emitter bismuth-212. The *in vivo* generator principle poses the additional challenge that the energetic decay process of the parent isotope (recoil energy and shower of conversion or Auger electrons) can induce dissociation, and the chelating system must be able to resist this or allow rapid reassociation with the daughter nuclide. Macrocyclic polyaminocarboxylate chelators, particularly DOTA (Fig. 4) show efficacy as bifunctional chelators of Pb^{2+} but it has been shown that replacing the carboxylate groups with primary amides, giving an octadentate ligand TCMC (**10**, Fig. 4) which coordinates through the four amines and four carbonyl oxygens of the amide groups, is advantageous and in use in a clinical trial of ^{212}Pb -labelled antibody.151–153

Group 15

Nitrogen-13 (β^+ , 99.8%, half life 10 min) is a very short-lived positron-emitting radionuclide most readily produced from cyclotrons in the form of ammonia or, less commonly, nitrate/nitrite. Its only established clinical application is use of $^{13}\text{NH}_3$ as a myocardial perfusion PET imaging agent. The ubiquitous appearance of nitrogen in biomolecules, metabolites and drugs creates attractive applications based on incorporating ^{13}N into more complex molecules, but this has been to all intents and purposes unrealised because of the perception that the half-life is too short for the relatively complex chemistry to be practicable. However, very recently the feasibility has been demonstrated to utilise $^{13}\text{NH}_3$ as a precursors for more complex molecules,154, 155 opening a potential new field of organic PET radiochemistry. Inorganic applications might also be envisaged utilising the ability of ammonia to bind to metals.

Phosphorus-32 (β^- , 100%, half-life 14 days), a high-energy beta-emitter, is the oldest radionuclide used in nuclear medicine, having been evaluated in the 1930s in the form of phosphate for treatment of haematological disorders. It is still used for treatment of polycythemia vera. It has also been widely used for palliative therapy of bone metastases, since it targets areas of bone mineral deposition, but has fallen out of favour because of high bone marrow dose associated with uptake in rapidly dividing cells in bone marrow. Its complete lack of photoemission precludes reliable imaging. Lack of imageable emissions has not prevented widespread therapeutic use of other beta-emitters such as ^{90}Y , however, and it is surprising that ^{32}P has barely been used therapeutically in any chemically targeted form other than phosphate and polyphosphates (except radiolabelled colloids for topical application in tumours and arthritis). Given its relatively low cost and an amenable half-life, it is possible to imagine that useful agents could be developed by broadening the chemistry, perhaps to incorporate ^{32}P into some of the many bisphosphonate drugs that are now widely used in treatment of bone diseases. The very few attempts to develop more complex targeted agents containing ^{32}P include labelling of ATP156 and labelling of targeting proteins.157 ^{33}P (β^- , 100%, half-life 25.3 days), a medium-energy beta-emitter, has been suggested as an alternative to ^{32}P as a therapeutic radionuclide with lower energy beta emissions,158 but no biological or clinical evaluations have been reported to date.

Arsenic has several positron emitting isotopes with potential for PET imaging including ^{71}As (β^+ , 30%, half-life 64 h), ^{72}As (β^+ , 88%, half-life 26 h), and ^{74}As (β^+ , 29%, half-life

17.8 days), and beta-emitting isotopes that in principle could be used for radionuclide therapy, including ^{77}As (β^- , 100%, half-life 38.8 h) and ^{76}As (β^- , 100%, half-life 26.3 h). The half-lives of all the positron emitters are compatible with use with antibody targeting. ^{72}As can be produced from a generator (parent isotope ^{72}Se)¹⁵⁹ by eluting it in the form of arsenic triiodide AsI_3 , which can be covalently attached to antibodies modified to create thiol side chains, by elimination of HI with formation of arsenic-sulfur bonds.¹⁶⁰ Although radionuclide imaging with ^{74}As dates back to the 1950s,¹⁶¹ it has been explored surprisingly little to date.

Bismuth-212 (α , 36%, β^- , 64%, half-life 60.6 min) and bismuth-213 (complex decay chain involving alpha and beta emissions, half-life 46 min) are alpha emitters. Their short half-lives are less than ideal for targeted radionuclide therapy but still, some targeting molecules may have sufficiently rapid target accumulation *in vivo* that they could be used. ^{213}Bi is eluted from the $^{225}\text{Ac}/^{213}\text{Bi}$ generator and is readily chelated by DOTA derivatives for attachment to antibodies; applications are envisaged in diffuse cancers in which the radiopharmaceutical can easily access individual cancer cells (e.g. leukaemias),¹⁶² or possibly using a pre-targeting approach using ^{213}Bi -conjugated biotin.¹⁶³ ^{212}Bi will most likely find application in the form of the *in vivo* generator whereby ^{212}Pb attached to a targeting molecule (see Group 14) decays *in vivo* to ^{212}Bi , which, if the chelate withstands the decay process, remains *in situ* long enough to deliver its alpha particles to the target tissue.^{151–153}

Group 16

The half-life of oxygen-15 (β^+ , 100%, half-life 2 min), which can be produced in cyclotrons in the form of H_2O (used for blood flow quantification) or O_2 , is so short that even die-hards who consider ^{15}N and ^{62}Cu amenable to incorporation into targeting molecules draw the line at labelling complex molecules with it. Nevertheless CO , butanol and 2-deoxy-D-glucose have been labelled for potential *in vivo* applications.¹⁶⁴

Group 17

Fluorine-18 (β^+ , 96.7%, half-life 20 min) is currently by far the most important radionuclide in PET, and is used most often in the form of [^{18}F]-2-fluoro-2-deoxyglucose. By far the major route to incorporating it into targeting molecules is formation of carbon-fluorine bonds, which falls outside the scope of this inorganic Perspective. However, interest in the inorganic chemistry of fluorine, using elements other than carbon as a binding site for ^{18}F , is growing. Since it has been reviewed recently¹⁶⁵ it will be introduced here very briefly. Boron, aluminium and silicon, all of which have very high bond energy in binding with fluorine, have been the most studied. ^{18}F -labelled aryl trifluoroborate (ArBF_3^-) and alkylfluorosilanes^{166, 167} have been used as prosthetic groups for labelling biomolecules, and the ^{18}F -labelled tetrafluoroborate ion is, like iodide (*vide infra*) and pertechnetate, a substrate of the sodium/iodide symporter and is under development as a PET imaging agent for thyroid disease, with the potential to improve on the sensitivity of gamma camera and SPET imaging with [$^{99\text{m}}\text{Tc}$]-pertechnetate (Fig. 18).^{168, 169} Coordinatively unsaturated aluminium complexes based on bifunctional NOTA derivatives can be linked to

biomolecules and will complex fluoride ions to produce stable radiopharmaceuticals. This is an exciting new area which has recently been reviewed.^{170, 171} With further development to introduce aluminium chelates that will bind fluoride under milder conditions and reach higher specific activity, it may have the potential to bring simple, one-step kit-like labelling chemistry to ^{18}F labelling of biomolecules.

Bromine has positron emitting isotopes ^{75}Br (half-life 96.7 min) and ^{76}Br (half-life 16.2 h) that can usefully be incorporated into organic molecules, usually by formation of aromatic C-Br bonds using oxidative electrophilic bromination. Much of this chemistry is analogous to iodination chemistry referred to below. Despite the suitable emission properties of the isotopes they have not found wide use. The production and utility of these isotopes have been reviewed recently.¹⁷²

Iodine isotopes are extremely versatile, both from a radiological and chemical perspective. Iodine-131 (β^- , 91%, γ , 82%, half-life 8.1 days) is of great historical significance in nuclear medicine and was among the earliest isotopes used clinically, originally used primarily as a radionuclide therapy in thyroid disease and later, with the advent of imaging, as an imaging agent for “thyroid function”. Its half-life is suitable for therapy in this context but its imaging characteristics are not ideal and better images, with smaller radiation doses, were later accessible with the introduction of the gamma-emitter ^{123}I (γ , 83%, half-life 13 h). In the age of PET, iodine is represented by ^{124}I (β^+ , 23%, half-life 4.2 days) which, despite less than ideal imaging properties and an unnecessarily long half-life, advances the sensitivity of imaging a step further compared to the gamma-emitting isotopes. As well as imaging “thyroid function” (later transforming into “molecular imaging” of sodium/iodide symporter activity once that transporter had been identified, cloned and characterised in the 1990s, nicely illustrating a semantic distinction between functional imaging and molecular imaging as different interpretations of the same imaging process in different eras), it is readily incorporated into organic and biological molecules, usually by formation of aromatic carbon-iodine bonds. In the case of proteins and peptides this is most often by electrophilic substitution in the activated aromatic groups of tyrosine side chains. The chemistry of incorporation of radioiodine into organic and biological molecules has been well-reviewed elsewhere.^{173–175}

Astatine-211 (α , 100%, half-life 7 h) is one of the prominent alpha-emitting radionuclides being evaluated for radionuclide therapy. It holds a fascination for many inorganic chemists, because, having no stable elements, its chemistry has barely been explored. Most of the chemistry for incorporating it into targeting molecules is based on an assumed analogy to iodine, with a tendency towards preferring higher oxidation states by comparison. Hence it is usually incorporated with reasonable stability into aromatic groups by C-At bond formation using electrophilic substitution.¹⁷³ However, it has recently been the subject of interest from an inorganic perspective, on the one hand being treated as a metal to see whether chelating agents could bind it satisfactorily in its higher oxidation states, and on the other by exploring the coordination of astatide ions to the softer transition metals. These approaches are at the very early stages of evaluation and have not yet shown signs of replacing conventional organic astatine chemistry as the basis of radiolabelling.^{176–180}

Group 18

Being “noble” the group 18 elements cannot be incorporated into targeting molecules but are useful in the form of the elemental gas for lung ventilation studies and perfusion of tissues, especially brain and liver. Gamma emitting members of the family are krypton-81m (γ , 68%, half-life 13 s),¹⁸¹ and xenon-133 (γ , 37%, β^- , 100%, half-life 5.24 days).²⁹ The gaseous state is exploited in the design of the krypton-81m generator, from which the gas is eluted from a solid support with air directly into the inhaled airstream.

Lanthanides

The coordination preferences of the lanthanides bear similarity to the group 3 and group 13 metals, and all form 3+ cations that can be chelated with oxygen/nitrogen donor ligands, with maximum kinetic stability obtained using macrocyclic ligands, especially DOTA. Although all can be effectively bound by the same chelator, there is a contraction in ionic radius towards the right of the period (the “lanthanide contraction”), which affects the coordination number, potentially leading to variations in biological behaviour when bioconjugates with the same chelator are labelled with different metals. Most important are lutetium-177 (β^- , 100%, γ , 14%, half-life 6.65 days),¹⁰ samarium-153 (β^- , 100%, γ , 29.8%, half-life 46.27 h),¹⁸² holmium-166 (β^- , 100%, half-life 1.12 days),¹⁸³ and terbium-149 (α , 16.7%, β^+ , 83.3%, half-life 4.12 h),¹⁸⁴ all of which are therapeutic isotopes and some of which can be imaged with a gamma or PET camera. The overlap in chemistry between the lanthanide elements and the group 3 and 13 metals is useful as a basis for multimodality imaging (aspects of which are discussed elsewhere in this issue), exploiting the luminescent properties of the elements for optical imaging, the high relaxivity of gadolinium complexes for magnetic resonance imaging, and the radionuclide properties of the lanthanides and chemically similar elements like ⁶⁸Ga and ¹¹¹In which can share the same chelators.

Actinides

Actinium-225 (α , complex decay chain, half-life 10.0 days) decays via a sequence of alpha-emissions and so imparts an extraordinarily high local radiation dose per atom, which can be exploited for targeted radionuclide therapy. Despite the large ionic radius, the well-established macrocyclic chelator DOTA is a satisfactory means for coupling Ac³⁺ to targeting molecules such as antibodies, and the DOTA complex is indeed more kinetically stable than complexes of related macrocyclic ligands of higher denticity.¹⁸⁵ Thorium-227 (α , complex decay chain, half-life 18.5 days) also decays via a sequence of alpha-emissions, and is also adequately bound to antibodies by DOTA-based bifunctional chelators.¹⁸⁶ These alpha-decay series elements are currently involved in a number of early-phase clinical trials with commercial sponsorship; it is a rapidly developing field, invigorated by the success of larger trials with ²²³Ra (see Group 2) in palliative treatment of bone metastases.

Conclusion

Nuclear medicine and molecular imaging has provided a gratifying mix of inorganic chemistry challenges, multidisciplinary collaboration, and tangible benefits to patients,

health services and business, making it a stimulating and hugely varied area in which to spend a career in inorganic chemistry and providing opportunities to apply chemistry not only from all areas of the periodic table, but different types of materials and molecules including organic molecules, metal chelates, proteins, peptides and nanoparticles. There have been significant developments recently in many of these areas, raising prospects for translation of new radionuclides and molecular imaging mechanisms, which in turn creates new inorganic chemical challenges. It will be interesting for inorganic chemists not only to observe the outcomes of their past developments for clinical applications and commercial products, but to drive them by providing new chemistry to improve the quality and accessibility of molecular imaging and radionuclide therapy for patients. Old challenges remain and new ones emerge across the periodic table. New non-cardiac applications should emerge for the ^{82}Rb generator. The ^{68}Ga generator is becoming established clinically as a source of positron emitting radiopharmaceuticals, with the possibility to revolutionise PET by making it available to centres without cyclotrons and complex radiochemistry facilities. To achieve this requires a shift in emphasis in chelator design from long-term kinetic stability towards rapid complexation under mild conditions and at very low concentration. New generator-produced medium-half-life positron emitting radionuclides such as ^{44}Sc and ^{90}Nb are emerging and may offer similar possibilities. All these isotopes require new chemistry for effective, and above all, simple incorporation into targeting molecules. Longer half life positron emitters such as ^{89}Zr isotopes are already making an impact in imaging with antibodies in humans, and this impact may now spread to cell tracking. The growing availability and versatility of very short half-life (<20 min) positron emitters (^{13}N , ^{62}Cu , ^{82}Rb , ^{15}O , $^{52\text{m}}\text{Mn}$) presents a new opportunity to perform multiple scans in individual patients to explore multiple facets of tissue physiology and gene expression in a single scanning session, without unduly high radiation doses; realisation of this possibility also creates needs and opportunities for innovative fast chemistry. The emergence of generator-produced positron emitters, and the closure of reactors producing ^{99}Mo , threatens the position of $^{99\text{m}}\text{Tc}$ at the centre of radionuclide imaging, but a renaissance of $^{99\text{m}}\text{Tc}$ may follow if the production infrastructure becomes more secure. This will highlight a need for new technetium chemistry, particularly for convenient kit-based incorporation into biomolecules, which despite many years of research remains far from optimal and $^{99\text{m}}\text{Tc}$ has surrendered a lead to ^{68}Ga in this respect. Copper radioisotopes continue to command very wide interest and there is a growing recognition of their potential in the study of copper biochemistry in health and disease, creating a major new field of activity in PET. The use of metals such as aluminium as binding sites for fluoride shows promise for easy incorporation of ^{18}F into biomolecules but this has some way to go to achieve its potential; this approach could be extended to other metals and radiolabels. Finally, the clinical success with ^{223}Ra radionuclide therapy may stimulate a resurgence of interest in radionuclide therapy, especially with alpha-emitting isotopes, e.g. of Bi, Ac, Th, Pb, At and Tb, whose coordination chemistry has yet to be optimised for the purpose, and of ^{223}Ra which requires completely new thinking if it is to be incorporated into biological targeting molecules. There is something for everyone.

Acknowledgment

I am grateful to many colleagues for the opportunity to include recent data and for reading and offering helpful advice on the manuscript. This research was supported by the Centre of Excellence in Medical Engineering Centre funded by the Wellcome Trust and EPSRC under grant number WT088641/Z/09/Z, and the King's College London and UCL Comprehensive Cancer Imaging Centre funded by CRUK and EPSRC in association with the MRC and DoH (England), and by the National Institute for Health Research (NIHR) Biomedical Research Centre at Guy's and St Thomas' NHS Foundation Trust and King's College London. PET and SPECT scanning equipment was funded by an equipment grant from the Wellcome Trust. The views expressed are those of the author(s) and not necessarily those of the NHS, the NIHR or the Department of Health.

Notes and references

1. Ghotbi AA, Kjaer A, Hasbak P. *Clin Physiol Functional Imaging*. 2014; 34:163.
2. Dickson JC, Endozo R, Erlandsson K, Wan S, Neriman D, Blower PJ, Groves AM. *J Nucl Med*. 2014 in press.
3. Lin A, Ray ME. *Cancer Metastasis Rev*. 2006; 25:669. [PubMed: 17160556]
4. Simpson WJ, Orange RP. *Can Med Assoc J*. 1965; 93:1237. [PubMed: 5839221]
5. Nilsson S, Larsen RH, Fosså SD, Balteskard L, Borch KW, Westlin JE, Salberg G, Bruland OS. *Clin Cancer Res*. 2005; 11:4451. [PubMed: 15958630]
6. Jauregui-Osoro M, Williamson PA, Galaria A, Sunassee K, Charoenphun P, Green MA, Mullen GED, Blower PJ. *Dalton Trans*. 2011; 40:6226. [PubMed: 21394352]
7. Price EW, Orvig C. *Chem Soc Rev*. 2014; 43:260. [PubMed: 24173525]
8. Koumariou E, Loktionova NS, Fellner M, Roesch F, Thews O, Pawlak D, Archimandritis SC, Mikolajczak R. *Appl Radiat Isot*. 2012; 70:2669. [PubMed: 23037921]
9. Majkowska-Pilip A, Bilewicz A. *J Inorg Biochem*. 2011; 105:313. [PubMed: 21194633]
10. Romer A, Seiler D, Marincek N, Brunner P, Koller MT, Ng QKT, Maecke HR, Mueller-Brand J, Rochlitz C, Briel M, Schindler C, et al. *Eur J Nucl Med Mol Imaging*. 2014; 41:214. [PubMed: 24085501]
11. Emmanouilides C. *Cancer Management Res*. 2009; 1:131.
12. Walrand S, Jamar F, Mathieu I, Camps J, Lonneux M, Sibomana M, Labar D, Michel C, Pauwels S. *Eur J Nucl Med Mol Imaging*. 2003; 30:354. [PubMed: 12634962]
13. Holland JP, Vasdev N. *Dalton Trans*. 2014; 43:9872. [PubMed: 24722728]
14. Rice SL, Roney CA, Daumar P, Lewis JS. *Semin Nucl Med*. 2011; 41:265. [PubMed: 21624561]
15. Vugts DJ, Visser GWM, van Dongen GAMS. *Current Topics Med Chem*. 2013; 13:446.
16. Deri MA, Zeglis BM, Francesconi LC, Lewis JS. *Nucl Med Biol*. 2013; 40:3. [PubMed: 22998840]
17. Heuveling DA, van Schie A, Vugts DJ, Hendrikse NH, Yaqub M, Hoekstra OS, Karagozoglou KH, Leemans CR, van Dongen GAMS, de Bree R. *J Nucl Med*. 2013; 54:585. [PubMed: 23378643]
18. Ma MT, Meszaros L, Berry DJ, Cooper M, Clark SJ, Ballinger JR, Blower PJ, Paterson BM, Ma Y, Hider RC. *J Biol Inorg Chem*. 2014; 19:S649.
19. Berry DJ, Ma Y, Ballinger JR, Tavaré R, Koers A, Sunassee K, Zhou T, Nawaz S, Mullen GED, Hider RC, Blower PJ. *Chem Commun*. 2011; 47:7068.
20. Deri MA, Ponnala S, Zeglis BM, Pohl G, Dannenberg JJ, Lewis JS, Francesconi LC. *J Med Chem*. 2014; 57:4849. [PubMed: 24814511]
21. Guerard F, Lee Y-S, Brechbiel MW. *Chem Eur J*. 2014; 20:5584. [PubMed: 24740517]
22. Guerard F, Lee Y-S, Tripier R, Szajek LP, Deschamps JR, Brechbiel MW. *Chem Commun*. 2013; 49:1002.
23. Patra M, Bauman A, Mari C, Fischer CA, Blacque O, Häussinger D, Gasser G, Mindt TL. *Chem Commun*. 2014; 50:11523.
24. Charoenphun P, Meszaros LK, Chuamsaamarkkee, Sharif-Paghaleh E, Ballinger JR, Ferris TJ, Went MJ, Mullen GED, Blower PJ. *Eur J Nucl Med Mol Imaging*. 2014; 41 submitted.
25. Radchenko V, Hauser H, Eisenhut M, Vugts DJ, van Dongen GAMS, Roesch F. *Radiochim Acta*. 2012; 100:857.

26. Lacy JL, Layne WW, Guidry GW, Verani MS, Roberts R. *J Nucl Med.* 1991; 32:2158. [PubMed: 1941155]
27. Buck A, Nguyen N, Burger C, Ziegler S, Frey L, Weigand G, Erhardt W, SenekowitschSchmidtke R, Pellikka R, Blauenstein P, Locher JT, et al. *Eur J Nucl Med.* 1996; 23:1619. [PubMed: 8929316]
28. Jain D. *Semin Nucl Med.* 1999; 29:221. [PubMed: 10433338]
29. Saha GB, Macintyre WJ, Go RT. *Semin Nucl Med.* 1994; 24:324. [PubMed: 7817203]
30. Peters AM. *Semin Nucl Med.* 1994; 24:110. [PubMed: 8023168]
31. Vanzetto G, Fagret D, Ghezzi C. *J Nucl Cardiol.* 2004; 11:647. [PubMed: 15592185]
32. Tisato F, Porchia M, Bolzati C, Refosco F, Vittadini A. *Coord Chem Rev.* 2006; 250:2034.
33. Banerjee S, Pillai MRA, Ramamoorthy N. *Semin Nucl Med.* 2001; 31:260. [PubMed: 11710769]
34. Johannsen B, Spies H. *Technetium and Rhenium.* 1996; 176:77.
35. Boschi A, Duatti A, Uccelli L. Development of technetium-99m and rhenium-188 radiopharmaceuticals containing a terminal metal-nitrido multiple bond for diagnosis and therapy. *Contrast Agents III: Radiopharmaceuticals - from Diagnostics to Therapeutics.* Krause W, editor. Springer; Berlin/Heidelberg: 2005. Topics in Current Chemistry series no. 252
36. Coogan MP, Doyle RP, Valliant JF, Babich JW, Zubieta J. *J Labelled Compd Radiopharm.* 2014; 57:255.
37. Kluba CA, Mindt TL. *Molecules.* 2013; 18:3206. [PubMed: 23481882]
38. Herman LW, Sharma V, Kronauge JF, Barbarics E, Herman LA, Piwnicaworms D. *J Med Chem.* 1995; 38:2955. [PubMed: 7636856]
39. Meszaros LK, Dose A, Biagini SCG, Blower PJ. *Inorg Chim Acta.* 2010; 363:1059.
40. Braband H, Benz M, Tooyama Y, Alberto R. *Chem Commun.* 2014; 50:4126.
41. Wullemmin MA, Stuber WT, Fox T, Reber MJ, Bruehwiler D, Alberto R, Braband H. *Dalton Trans.* 2014; 43:4260. [PubMed: 24326345]
42. van Noorden R. *Nature.* 2013; 504:202. [PubMed: 24336269]
43. King RC, Surfraz MB-U, Biagini SCG, Blower PJ, Mather SJ. *Dalton Trans.* 2007:4998. [PubMed: 17992285]
44. Wang Y, Liu X, Hnatowich DJ. *Nature Protocols.* 2007; 2:972. [PubMed: 17446896]
45. Huber GJ, Alberto RA, Blauenstein P, Anderegg G. *J Chem Soc Chem Commun.* 1989:879.
46. Abiraj K, Mansi R, Tamma M-L, Forrer F, Cescato R, Reubi JC, Akyel KG, Maecke HR. *Chem Eur J.* 2010; 16:2115. [PubMed: 20066690]
47. Choudhry U, Greenland WEP, Goddard WA, MacLennan TAJ, Teat SJ, Blower PJ. *Dalton Trans.* 2003:311.
48. Hofstrom C, Altai M, Honarvar H, Strand J, Malmberg J, Hosseinimehr SJ, Orlova A, Graslund T, Tolmachev V. *J Med Chem.* 2013; 56:4966. [PubMed: 23692562]
49. Tolmachev V, Hofstrom C, Malmberg J, Ahlgren S, Hosseinimehr SJ, Sandstrom M, Abrahmsen L, Orlova A, Graslund T. *Bioconjugate Chem.* 2010; 21:2013.
50. Badar A, Williams J, de Rosales RT, Tavare R, Kampmeier F, Blower PJ, Mullen GE. *Eur J Nucl Med Mol Imaging Res.* 2014; 4:14.
51. Tavare R, De Rosales RTM, Blower PJ, Mullen GED. *Bioconjugate Chem.* 2009; 20:2071.
52. Tavare R, Williams J, Howland K, Blower PJ, Mullen GED. *J Inorg Biochem.* 2012; 114:24. [PubMed: 22687562]
53. Williams JD, Cooper M, Kampmeier F, Tavare R, Mullen GE, Blower P. *Eur J Nucl Med Mol Imaging.* 2012; 39:S216.
54. Pasqualini R, Duatti A. *J Chem Soc Chem Commun.* 1992:1354.
55. Pasqualini R, Duatti A, Bellande E, Comazzi V, Brucato V, Hoffschir D, Fagret D, Comet M. *J Nucl Med.* 1994; 35:334. [PubMed: 8295007]
56. Berry DJ, de Rosales RTM, Charoenphun P, Blower PJ. *Mini-Rev Med Chem.* 2012; 12:1174. [PubMed: 22931590]
57. Carta D, Jentschel C, Thieme S, Salvarese N, Morellato N, Refosco F, Ruzza P, Bergmann R, Pietzsch H-J, Bolzati C. *Nucl Med Biol.* 2014; 41:570. [PubMed: 24909864]

58. Gomez Blanco N, Jauregui-Osoro M, Cobaleda-Siles M, Maldonado CR, Henriksen-Lacey M, Padro D, Clark S, Mareque-Rivas JC. *Chem Commun.* 2012; 48:4211.
59. Maldonado CR, Gomez-Blanco N, Jauregui-Osoro M, Brunton VG, Yate L, Mareque-Rivas JC. *Chem Commun.* 2013; 49:3985.
60. Torres Martin de Rosales R, Tavares R, Glaria A, Varma G, Protti A, Blower PJ. *Bioconjugate Chem.* 2011; 22:455.
61. Torres Martin de Rosales R, Blower PJ. The role of ^{99m}Tc in the development of rhenium radiopharmaceuticals. *Technetium radiopharmaceuticals: status and prospective.* Duatti A, editor IAEA; Vienna: 2008. 250–278.
62. Torres Martin de Rosales R, Finucane C, Mather SJ, Blower PJ. *Chem Commun.* 2009:4847.
63. Blower PJ, Kettle AG, O'Doherty MJ, Coakley AJ, Knapp FF. *Eur J Nucl Med.* 2000; 27:1405.
64. Mueller C, Schubiger PA, Schibli R. *Nucl Med Biol.* 2007; 34:595. [PubMed: 17707798]
65. Bruehlmeier M, Leenders KL, Vontobel P, Calonder C, Antonini A, Weindl A. *J Nucl Med.* 2000; 41:781. [PubMed: 10809192]
66. Beshara S, Sorensen J, Lubberink M, Tolmachev V, Langstrom B, Antoni G, Danielson BG, Lundqvist H. *Brit J Haematol.* 2003; 120:853. [PubMed: 12614222]
67. Srivastava SC, Richards P, Som P, Meinken G, Atkins HL, Sewatkar A, Ku TH. Ruthenium-97-labeled compounds - a new class of radiopharmaceuticals. *Frontiers in Nuclear Medicine.* Horst W, et al., editors Springer-Verlag; Berlin Heidelberg: 1980.
68. De Reuck J, Vonck K, Santens P, Boon P, De Bleecker J, Strijckmans K, Lemahieu I. *J Neurolog Sci.* 2000; 181:13.
69. Ferreira CL, Lapi S, Steele J, Green DE, Ruth TJ, Adam MJ, Orvig C. *Appl Radiat Isot.* 2007; 65:1303. [PubMed: 17666190]
70. Schmaljohann J, Karanikas G, Sinzinger H. *J Labelled Compd Radiopharm.* 2001; 44:395.
71. Akgun Z, Engelbrecht H, Cutler CS, Barnes CL, Jurisson SS, Lever SZ. *J Labelled Compd Radiopharm.* 2005; 48:S299.
72. Ballard BD, Kannan R, Katti KV, Hoffman T, Engelbrecht HP, Cutler CS, Jurisson SS. *J Labelled Compd Radiopharm.* 2005; 48:S19.
73. Goswami N, Higginbotham C, Volkert W, Alberto R, Nef W, Jurisson S. *Nucl Med Biol.* 1999; 26:951. [PubMed: 10708310]
74. Zweit J, Carnochan P, Goodall R, Ott R. *J Nucl Biol Med.* 1994; 38:18.
75. Nielsen GD, Andersen O, Jensen M. *Fund Appl Toxicol.* 1993; 21:236.
76. Packard AB, Spaeth K, Kronauge JF, Mirzadeh S. *J Labelled Compd Radiopharm.* 1997; 40:354.
77. Blower PJ, Lewis JS, Zweit J. *Nucl Med Biol.* 1996; 23:957. [PubMed: 9004284]
78. Shokeen M, Anderson CJ. *Acc Chem Res.* 2009; 42:832. [PubMed: 19530674]
79. Anderson CJ, Ferdani R. *Cancer Biother Radiopharm.* 2009; 24:379. [PubMed: 19694573]
80. Cai Z, Anderson CJ. *J Labelled Compd Radiopharm.* 2014; 57:224.
81. Holland JP, Lewis JS, Dehdashti F. *Quart J Nucl Med Mol Imaging.* 2009; 53:193.
82. Vavere AL, Lewis JS. *Dalton Trans.* 2007:4893. [PubMed: 17992274]
83. Hueting R. *J Labelled Compd Radiopharm.* 2014; 57:231.
84. Ma MT, Karas JA, White JM, Scanlon D, Donnelly PS. *Chem Commun.* 2009:3237.
85. Di Bartolo N, Sargeson AM, Smith SV. *Org Biomol Chem.* 2006; 4:3350. [PubMed: 17036125]
86. Ma MT, Cooper MS, Paul RL, Shaw KP, Karas JA, Scanlon D, White JM, Blower PJ, Donnelly PS. *Inorg Chem.* 2011; 50:6701. [PubMed: 21667932]
87. Cooper MS, Ma MT, Sunassee K, Shaw KP, Williams JD, Paul RL, Donnelly PS, Blower PJ. *Bioconjugate Chem.* 2012; 23:1029.
88. Silversides JD, Smith R, Archibald SJ. *Dalton Trans.* 2011; 40:6289. [PubMed: 21455520]
89. Lima LMP, Halime Z, Marion R, Camus N, Delgado R, Platas-Iglesias C, Tripiet R. *Inorg Chem.* 2014; 53:5269. [PubMed: 24758339]
90. Roosenburg S, Sosabowski JK, Joosten L, Cooper MS, Kolenc-Peit PK, Foster J, Burnet J, Oyen WJG, Blower PJ, Mather SJ, Boerman OC, et al. *Mol Pharm.* in press.

91. Dearling JLJ, Lewis JS, McCarthy DW, Welch MJ, Blower PJ. *Chem Commun.* 1998;2531.
92. Dearling JLJ, Lewis JS, Muller GED, Welch MJ, Blower PJ. *J Biol Inorg Chem.* 2002; 7:249. [PubMed: 11935349]
93. Maurer RI, Blower PJ, Dilworth JR, Reynolds CA, Zheng YF, Mullen GED. *J Med Chem.* 2002; 45:1420. [PubMed: 11906283]
94. Mullen GE, Zheng Y, Reynolds CA, Blower PJ, Dilworth JR. *J Nucl Med.* 2000; 41:123P. [PubMed: 10647615]
95. Huetting R, Kersemans V, Cornelissen B, Tredwell M, Hussien K, Christlieb M, Gee AD, Passchier J, Smart SC, Dilworth JR, Gouverneur V, et al. *J Nucl Med.* 2014; 55:128. [PubMed: 24337603]
96. Burgman P, O'Donoghue JA, Lewis JS, Welch MJ, Humm JL, Ling CC. *Nucl Med Biol.* 2005; 32:623. [PubMed: 16026709]
97. Donnelly PS, Liddell JR, Lim S, Paterson BM, Cater MA, Savva MS, Mot AI, James JL, Trounce IA, White AR, Crouch PJ. *Proc Nat Acad Sci USA.* 2012; 109:47. [PubMed: 22173633]
98. Price KA, Crouch PJ, Volitakis I, Paterson BM, Lim S, Donnelly PS, White AR. *Inorg Chem.* 2011; 50:9594. [PubMed: 21882803]
99. Griessinger CM, Kehlbach R, Bukala D, Wiehr S, Bantleon R, Cay F, Schmid A, Braumueller H, Fehrenbacher B, Schaller M, Eichner M, et al. *J Nucl Med.* 2014; 55:301. [PubMed: 24434289]
100. Huang J, Lee CCI, Sutcliffe JL, Cherry SR, Tarantal AF. *Mol Imaging.* 2008; 7:1. [PubMed: 18384718]
101. Charoenphun P, Paul R, Weeks A, Berry D, Shaw K, Mullen G, Ballinger J, Blower PJ. *Eur J Nucl Med Mol Imaging.* 2011; 38:S294.
102. Bhargava KK, Gupta RK, Nichols KJ, Palestro CJ. *Nucl Med Biol.* 2009; 36:545. [PubMed: 19520295]
103. Dearling JLJ, Mullen GED, Lewis JS, Welch MJ, Blower PJ. *J Labelled Compd Radiopharm.* 1999; 42:S276.
104. Fodero-Tavoletti MT, Villemagne VL, Paterson BM, White AR, Li Q-X, Camakaris J, O'Keefe GJ, Cappai R, Barnham KJ, Donnelly PS. *J Alzheimers Disease.* 2010; 20:49. [PubMed: 20164590]
105. Bagunya-Torres J, Andreozi E, Blower PJ. submitted
106. Qin C, Liu H, Chen K, Hu X, Ma X, Lan X, Zhang Y, Cheng Z. *J Nucl Med.* 2014; 55:812. [PubMed: 24627435]
107. Handley MG, Medina RA, Mariotti E, Kenny GD, Shaw KP, Yan R, Eykyn TR, Blower PJ, Southworth R. *J Nucl Med.* 2014; 55:488. [PubMed: 24421288]
108. Ng Y, Lacy JL, Fletcher JW, Green MA. *Appl Radiat Isot.* 2014; 91:38. [PubMed: 24886964]
109. Betts HM, Barnard PJ, Bayly SR, Dilworth JR, Gee AD, Holland JP. *Angew Chem Int Ed.* 2008; 47:8416.
110. Sun X, Huang X, Guo J, Zhu W, Ding Y, Niu G, Wang A, Kiesewetter DO, Wang ZL, Sun S, Chen X. *J Amer Chem Soc.* 2014; 136:1706. [PubMed: 24401138]
111. Wong RM, Gilbert DA, Liu K, Louie AY. *ACS Nano.* 2012; 6:3461. [PubMed: 22417124]
112. Zeng D, Lee NS, Liu Y, Zhou D, Dence CS, Wooley KL, Katzenellenbogen JA, Welch MJ. *ACS Nano.* 2012; 6:5209. [PubMed: 22548282]
113. Torres Martin de Rosales R, Tavare R, Paul RL, Jauregui-Osoro M, Protti A, Glaria A, Varma G, Szanda I, Blower PJ. *Angew Chem Int Ed.* 2011; 50:5509.
114. Alberto R, Blauenstein P, Novakhofer I, Smith A, Schubiger PA. *Appl Radiat Isot.* 1992; 43:869.
115. Berning DE, Katti KV, Volkert WA, Higginbotham CJ, Ketring AR. *Nucl Med Biol.* 1998; 25:577. [PubMed: 9751426]
116. Gadbois WF, Corriere JN. *J Urol.* 1974; 112:420. [PubMed: 4416575]
117. Blower PJ, Smith RJ, Jolley C. *Nucl Med Commun.* 1992; 13:231.
118. Draisma A, Maffioli L, Gasparini M, Savelli G, Pauwels E, Bombardieri E. *Tumori.* 1998; 84:434. [PubMed: 9824994]
119. Even-Sapir E, Israel O. *Eur J Nucl Med Mol Imaging.* 2003; 30:S65. [PubMed: 12644887]
120. Goldsmith SJ, Vallabhajosula S. *Semin Nucl Med.* 2009; 39:2. [PubMed: 19038596]

121. Weiner RE. Nucl Med Biol. 1996; 23:745. [PubMed: 8940716]
122. Jonkhoff AR, Huijgens PC, Versteegh RT, Vandieren EB, Ossenkoppele GJ, Martens HJM, Teule GJJ. Brit J Cancer. 1993; 67:693. [PubMed: 8471427]
123. Jonkhoff AR, Huijgens PC, Versteegh RT, Vanlingen A, Ossenkoppele GJ, Drager AM, Teule GJJ. Leukemia Res. 1995; 19:169. [PubMed: 7700078]
124. Jonkhoff AR, Plaizier M, Ossenkoppele GJ, Teule GJJ, Huijgens PC. Brit J Cancer. 1995; 72:1541. [PubMed: 8519674]
125. Michel RB, Brechbiel MW, Mattes MJ. J Nucl Med. 2003; 44:632. [PubMed: 12679410]
126. Ochakovskaya R, Osorio L, Goldenberg DM, Mattes MJ. Clin Cancer Res. 2001; 7:1505. [PubMed: 11410483]
127. Othman MF, Cooper M, Blower PJ, Lewington V. Eur J Nucl Med Mol Imaging. 2014 in press.
128. Banerjee SR, Pomper MG. Appl Radiat Isotopes. 2013; 76:2.
129. Velikyan I. Theranostics. 2014; 4:47.
130. Fellner M, Baum RP, Kubicek V, Hermann P, Lukes I, Prasad V, Roesch F. Eur J Nucl Med Mol Imaging. 2010; 37:834. [PubMed: 20069291]
131. Meckel M, Fellner M, Thieme N, Bergmann R, Kubicek V, Roesch F. Nucl Med Biol. 2013; 40:823. [PubMed: 23915801]
132. Fani M, Tamma M-L, Nicolas GP, Lasri E, Medina C, Raynal I, Port M, Weber WA, Maecke HR. Mol Pharm. 2012; 9:1136. [PubMed: 22497506]
133. Mathias CJ, Lewis MR, Reichert DE, Laforest R, Sharp TL, Lewis JS, Yang ZF, Waters DJ, Snyder PW, Low PS, Welch MJ, et al. Nucl Med Biol. 2003; 30:725. [PubMed: 14499330]
134. Burke BP, Clemente GS, Archibald SJ. J Labelled Compd Radiopharm. 2014; 57:239.
135. Afshar-Oromieh A, Zechmann CM, Malcher A, Eder M, Eisenhut M, Linhart HG, Holland-Letz T, Hadaschik BA, Giesel FL, Debus J, Haberkorn U. Eur J Nucl Med Mol Imaging. 2014; 41:11. [PubMed: 24072344]
136. Hoffer PB, Samuel A, Bushberg JT, Thakur M. Radiol. 1979; 131:775.
137. Hoffer PB, Samuel A, Bushberg JT, Thakur M. J Nucl Med. 1979; 20:248. [PubMed: 24180048]
138. Blower PJ, Cooper MS, Nawaz S, O'Neill A, Koers A, Sunassee K, Berry DJ, Mullen GED, Ballinger JR. Eur J Nucl Med Mol Imaging. 2012; 39:S262.
139. Petrik M, Franssen GM, Haas H, Laverman P, Hoertnagl C, Schrettl M, Helbok A, Lass-Floerl C, Decristoforo C. Eur J Nucl Med Mol Imaging. 2012; 39:1175. [PubMed: 22526953]
140. Petrik M, Haas H, Dobrozemsky G, Lass-Floerl C, Helbok A, Blatzer M, Dietrich H, Decristoforo C. J Nucl Med. 2010; 51:639. [PubMed: 20351354]
141. Petrik M, Haas H, Laverman P, Schrettl M, Franssen GM, Blatzer M, Decristoforo C. Mol Imaging Biol. 2014; 16:102. [PubMed: 23818006]
142. Petrik M, Haas H, Schrettl M, Helbok A, Blatzer M, Decristoforo C. Nucl Med Biol. 2012; 39:361. [PubMed: 22172389]
143. Bomanji JB, Papathanasiou ND. Eur J Nucl Med Mol Imaging. 2012; 39:113. [PubMed: 22009380]
144. Virgolini I, Britton K, Buscombe J, Moncayo R, Paganelli G, Riva P. Semin Nucl Med. 2002; 32:148. [PubMed: 11965610]
145. Malmberg J, Tolmachev V, Orlova A. Exp Ther Med. 2011; 2:523. [PubMed: 22977535]
146. Peters AM. Quart J Nucl Med Mol Imaging. 2005; 49:304.
147. Pagnanelli RA, Basso DA. J Nucl Med Technol. 2010; 38:1. [PubMed: 20159930]
148. Deutsch E, Bushong W, Glavan KA, Elder RC, Sodd VJ, Scholz KL, Fortman DL, Lukes SJ. Science. 1981; 214:85. [PubMed: 6897930]
149. Beller GA, Watson DD. Semin Nucl Med. 1991; 21:173. [PubMed: 1835136]
150. Bishayee A, Rao DV, Srivastava SC, Bouchet LG, Bolch WE, Howell RW. J Nucl Med. 2000; 41:2043. [PubMed: 11138691]
151. Baidoo KE, Milenic DE, Brechbiel MW. Nucl Med Biol. 2013; 40:592. [PubMed: 23602604]
152. Kim Y-S, Brechbiel MW. Tumor Biol. 2012; 33:573.
153. Yong K, Brechbiel MW. Dalton Trans. 2011; 40:6068. [PubMed: 21380408]

154. Gomez-Vallejo V, Gaja V, Gona KB, Llop J. *J Labelled Compd Radiopharm.* 2014; 57:244.
155. Blower JE, Cousin SF, Gee AD. submitted
156. Cheng Y, Senthamizhchelvan S, Agarwal R, Green GM, Mease RC, Sgouros G, Huso DL, Pomper MG, Meltzer SJ, Abraham JM. *Cell Cycle.* 2012; 11:1878. [PubMed: 22544324]
157. Patrick MR, Chester KA, Pietersz GA. *Cancer Immunol Immunother.* 1998; 46:229. [PubMed: 9671146]
158. Goddu SM, Bishayee A, Bouchet LG, Bolch WE, Rao DV, Howell RW. *J Nucl Med.* 2000; 41:941. [PubMed: 10809212]
159. Jennewein M, Qaim SM, Kulkarni RV, Mason RP, Hermanne A, Rosch F. *Radiochim Acta.* 2005; 93:579.
160. Jennewein M, Lewis MA, Zhao D, Tsyganov E, Slavine N, He J, Watkins L, Kodibagkar VD, O'Kelly S, Kulkarni P, Antich PP, et al. *Clin Cancer Res.* 2008; 14:1377. [PubMed: 18316558]
161. Sweet WH, Brownell GL. *J Amer Med Assoc.* 1955; 157:1183. [PubMed: 14353655]
162. Rosenblat TL, McDevitt MR, Mulford DA, Pandit-Taskar N, Divgi CR, Panageas KS, Heaney ML, Chanel S, Morgenstern A, Sgouros G, Larson SM, et al. *Clin Cancer Res.* 2010; 16:5303. [PubMed: 20858843]
163. Pagel JM, Kenoyer AL, Back T, Hamlin DK, Wilbur DS, Fisher DR, Park SI, Frayo S, Axtman A, Orgun N, Orozco J, et al. *Blood.* 2011; 118:703. [PubMed: 21613259]
164. Miller PW, Long NJ, Vilar R, Gee AD. *Angew Chem Int Ed.* 2008; 47:8998.
165. Smith GE, Sladen HL, Biagini SCG, Blower PJ. *Dalton Trans.* 2011; 40:6196. [PubMed: 21499604]
166. Kostikov AP, Chin J, Orchowski K, Niedermoser S, Kovacevic MM, Aliaga A, Jurkschat K, Waengler B, Waengler C, Wester H-J, Schirmacher R. *Bioconjugate Chem.* 2012; 23:106.
167. Waengler C, Niedermoser S, Chin J, Orchowski K, Schirmacher E, Jurkschat K, Iovkova-Berends L, Kostikov AP, Schirmacher R, Waengler B. *Nature Protocols.* 2012; 7:1946. [PubMed: 23037309]
168. Jauregui-Osoro M, Sunassee K, Weeks AJ, Berry DJ, Paul RL, Cleij M, Banga JP, O'Doherty MJ, Marsden PK, Clarke SEM, Ballinger JR, et al. *Eur J Nucl Med Mol Imaging.* 2010; 37:2108. [PubMed: 20577737]
169. Weeks AJ, Jauregui-Osoro M, Cleij M, Blower JE, Ballinger JR, Blower PJ. *Nucl Med Commun.* 2011; 32:98. [PubMed: 21085047]
170. Laverman P, McBride WJ, Sharkey RM, Goldenberg DM, Boerman OC. *J Labelled Compd Radiopharm.* 2014; 57:219.
171. McBride WJ, Sharkey RM, Goldenberg DM. *Eur J Nucl Med Mol Imaging Res.* 2013; 3:36.
172. Tolmachev V. *Curr Radiopharm.* 2011; 4:76. [PubMed: 22191647]
173. Adam MJ, Wilbur DS. *Chem Soc Rev.* 2005; 34:153. [PubMed: 15672179]
174. Seevers RH, Counsell RE. *Chem Rev.* 1982; 82:575.
175. Wilbur DS. *Bioconjugate Chem.* 1992; 3:433.
176. Champion J, Alliot C, Huclier S, Deniaud D, Asfari Z, Montavon G. *Inorg Chim Acta.* 2009; 362:2654.
177. Guerard F, Rajerison H, Faivre-Chauvet A, Barbet J, Meyer GJ, Haddad F, Da Silva I, Gestin JF. *Eur J Nucl Med Mol Imaging.* 2010; 37:S361.
178. Pruszyński M, Bilewicz A, Zalutsky MR. *Bioconjugate Chem.* 2008; 19:958.
179. Rajerison H, Guerard F, Mougín-Degraef M, Bourgeois M, Da Silva I, Cherel M, Barbet J, Faivre-Chauvet A, Gestin J-F. *Nucl Med Biol.* 2014; 41(Suppl):e23. [PubMed: 24661351]
180. Wilbur DS, Chyan M-K, Hamlin DK, Perry MA. *Bioconjugate Chem.* 2009; 20:591.
181. Lambrecht RM, Tomiyoshi K, Sekine T. *Radiochim Acta.* 1997; 77:103.
182. Anderson P, Nunez R. *Expert Rev Anticancer Ther.* 2007; 7:1517. [PubMed: 18020921]
183. Thompson S, Ballard B, Jiang Z, Revskaya E, Sisay N, Miller WH, Cutler CS, Dadachova E, Francesconi LC. *Nucl Med Biol.* 2014; 41:276. [PubMed: 24533987]
184. Beyer GJ, Miederer M, Vranjes-duric S, Comor JJ, Kunzi G, Hartley O, Senekowitsch-Schmidtke R, Soloviev D, Buchegger F. *Eur J Nucl Med Mol Imaging.* 2004; 31:547. [PubMed: 14722680]

185. Miederer M, Scheinberg DA, McDevitt MR. *Adv Drug Deliv Rev.* 2008; 60:1371. [PubMed: 18514364]
186. Abbas N, Bruland OS, Brevik EM, Dahle J. *Nucl Med Commun.* 2012; 33:838. [PubMed: 22643311]

1 H	2 He																
3 Li	4 Be											5 B	6 C β^+	7 N β^+	8 O β^+	9 F β^+	10 Ne
11 Na	12 Mg											13 Al	14 Si	15 P T	16 S	17 Cl	18 Ar
19 K	20 Ca	21 Sc β^+T	22 Ti	23 V	24 Cr	25 M β^+	26 Fe β^+	27 Co β^+	28 Ni β^+	29 Cu β^+T	30 Zn	31 Ga $\gamma\beta^+T$	32 Ge	33 As β^+	34 Se γ	35 Br β^+T	36 Kr γ
37 Rb β^+	38 Sr β^+T	39 Y β^+T	40 Zr β^+	41 Nb β^+	42 Mo	43 Tc $\gamma\beta^+$	44 Ru γ	45 Rh T	46 Pd	47 Ag T	48 Cd	49 In γ	50 Sn T	51 Sb	52 Te γ	53 I $\gamma\beta^+T$	54 Xe γ
55 Cs	56 Ba	57 La	72 Hf	73 Ta γ	74 W	75 Re T	76 Os	77 Ir	78 Pt γT	79 Au T	80 Hg T	81 Tl γ	82 Pb T	83 Bi T	84 Po	85 At T	86 Rn
87 Fr	88 Ra T	89 Ac T															
lanthanides	58 Ce	59 Pr	60 Nd	61 Pm	62 Sm T	63 Eu	64 Gd	65 Tb T	66 Dy	67 Ho T	68 Er	69 Tm	70 Yb	71 Lu T			
actinides	90 Th T	91 Pa	92 U	93 Np	94 Pu	95 Am	96 Cm	97 Bk	98 Cf	99 Es	100 Fm	101 Md	102 No	103 Lr			

Figure 1.

Periodic table highlighting (shaded) elements with radionuclides with uses or identified potential uses in molecular imaging or targeted radionuclide therapy. Main uses are identified by symbols: γ (gamma camera imaging/SPET), β^+ (positron emission tomography) and T (therapy, using beta-, alpha, or Auger-emitting radioisotopes). Some unshaded elements also have indirect importance e.g. as parent radionuclides for directly-used radionuclides, or as cyclotron target materials, or chemical binding sites for biomolecule labelling, hence the “usefulness” is somewhat arbitrary.

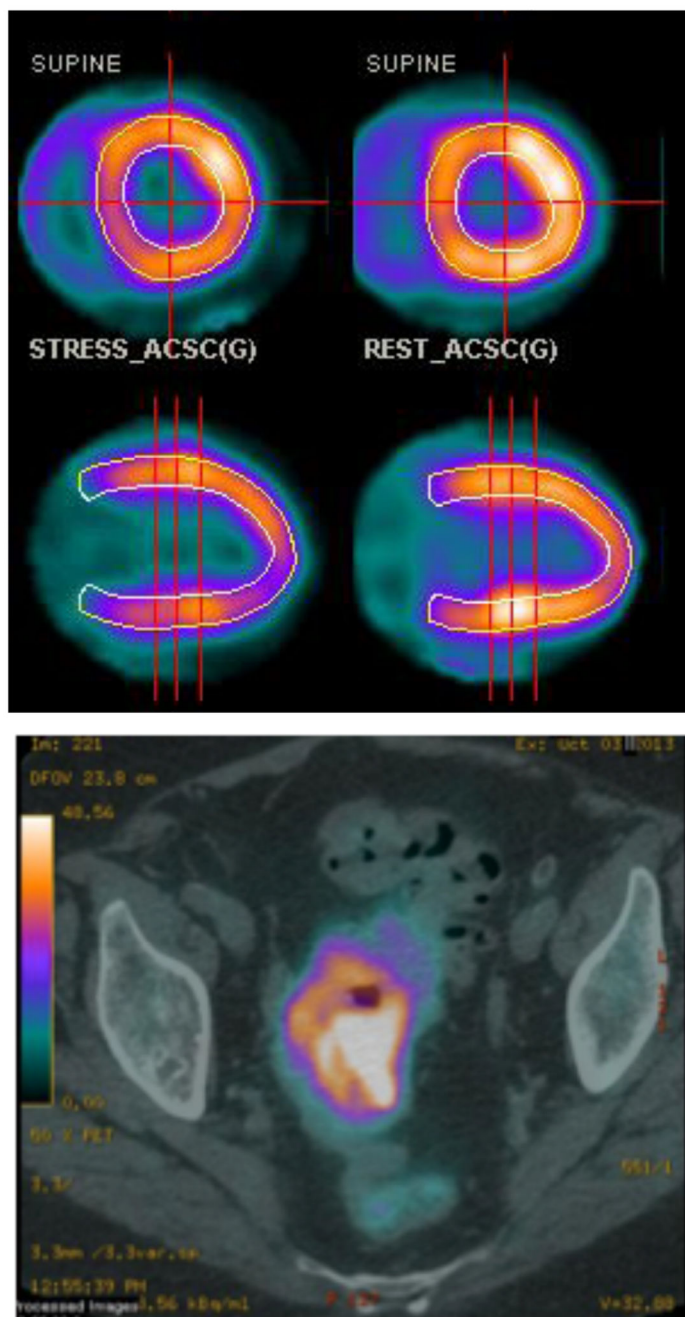
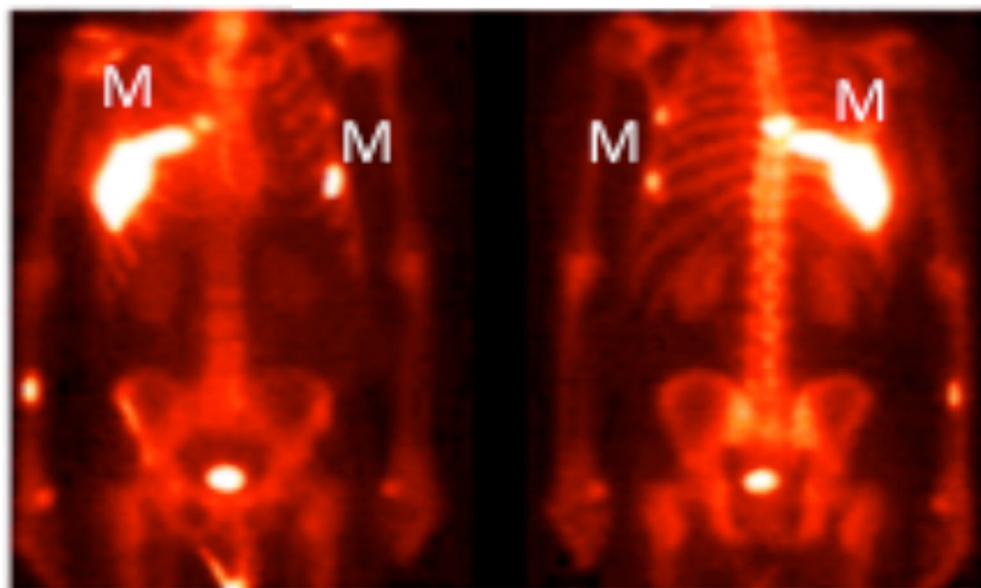
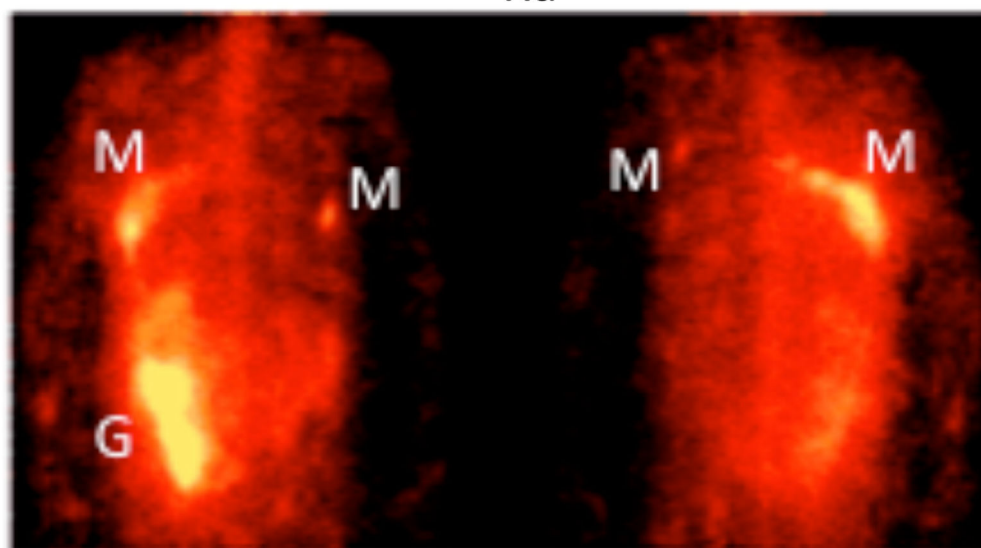


Figure 2.

Top: Example of myocardial perfusion PET imaging using $^{82}\text{Rb}^+$ (transverse (top) and sagittal (bottom) sections); bottom: PET-CT scan (transverse section, pelvic region) of a patient with colorectal cancer after injection of $^{82}\text{Rb}^+$. (Images courtesy of Prof A. M. Groves, University College London Hospitals)

^{99m}Tc bone scan ^{223}Ra **Figure 3.**

Biodistribution of ^{223}Ra in a patient with metastatic prostate cancer after i.v. administration of $^{223}\text{RaCl}_2$. The anterior (left) and posterior (right) views show specific uptake in the sites of bone metastases indicated by the ^{99m}Tc bone scan (M), and activity in the gut (G) indicating radioactivity that has undergone hepatobiliary excretion. The gamma camera image was possible by virtue of a low abundance gamma emission from ^{223}Ra accompanying the alpha decay. (Adapted with permission from ref. 5).

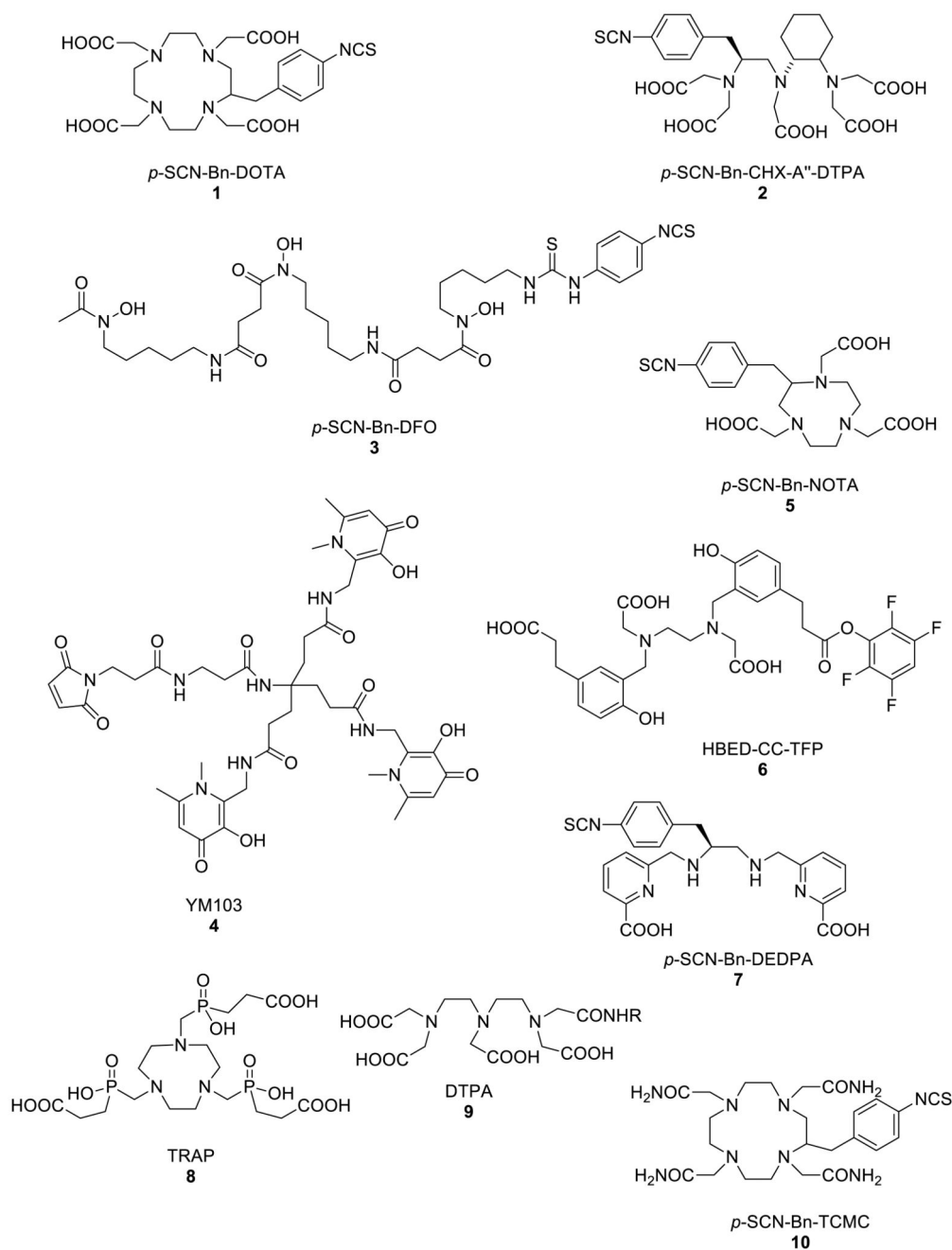


Figure 4.
Structures of bifunctional chelators used for radioactive di-, tri- and tetravalent metal ions

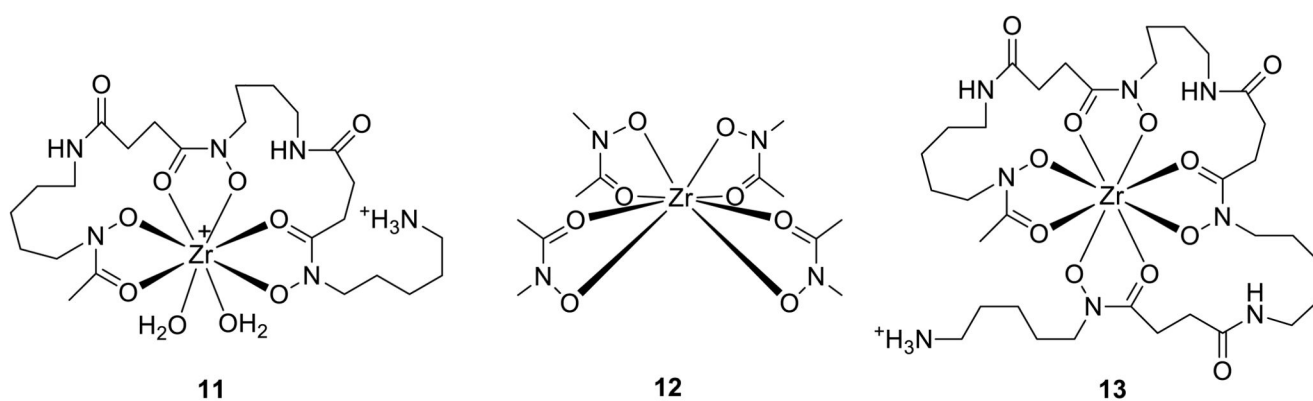


Figure 5. Left: Modelled coordination of Zr^{4+} by DFO (**11**);²⁰ Centre: Schematic structure of ZrL_4 (HL = *N*-methylacetohydroxamic acid) (**12**), serving as a template for the design of new octadentate chelators for Zr^{4+} (note that disorder in the C and N orientations of the hydroxamate rings precludes determination of their preferred relative orientation and suggests that any such preferences are weak);²² Right: Schematic structure of Zr^{4+} complex **13** of an octadentate DFO homologue.²³

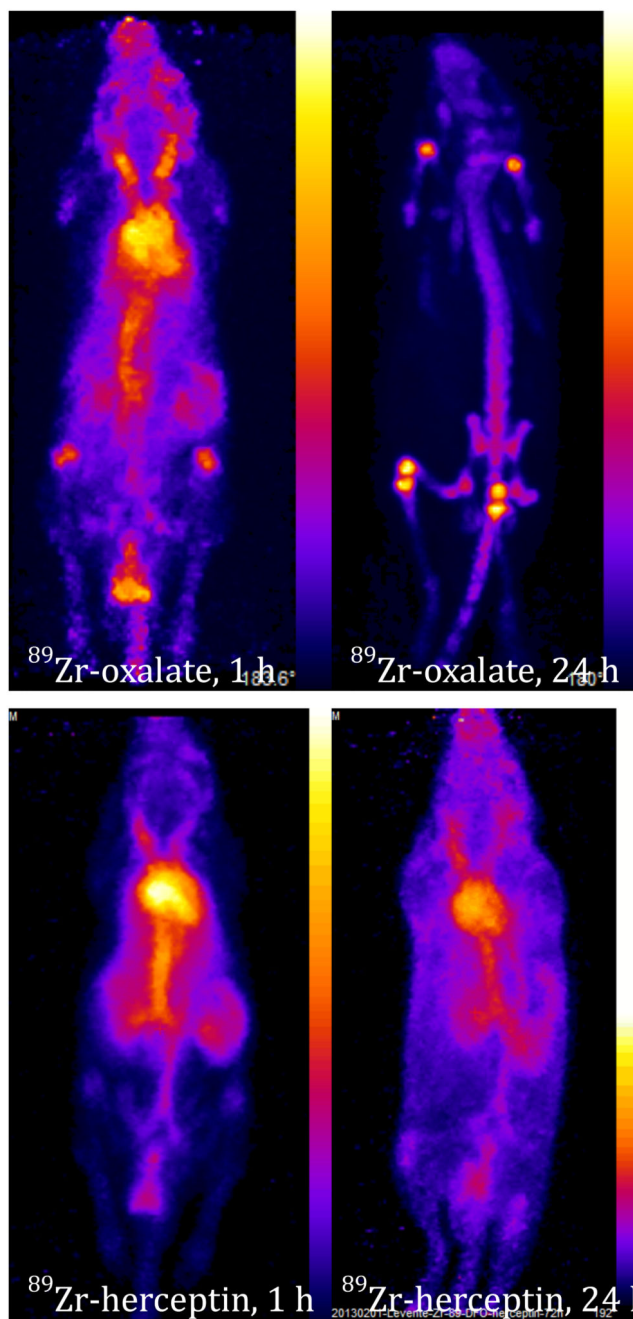


Figure 6. PET images showing biodistribution of ^{89}Zr -oxalate complex (top) and ^{89}Zr -labelled trastuzumab-DFO conjugate (bottom) at 1 h (left) and 4 h (right) post-injection in mice. Oxalate complex is gradually cleared from blood to bone and to some extent excreted through kidney, while the labelled antibody remains largely in the blood pool until at least 24 h, with only slight uptake in bone by 24 h.

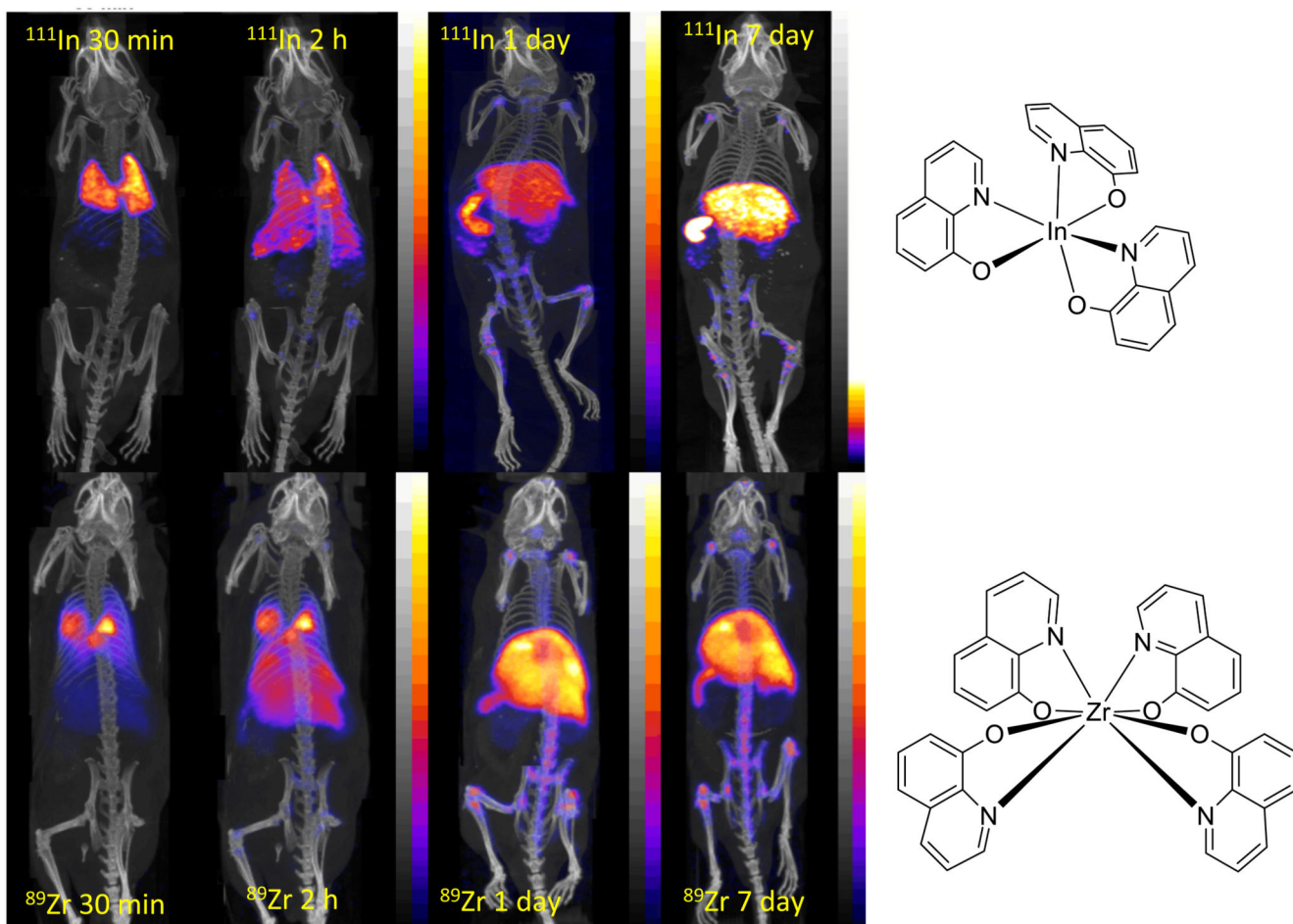


Figure 7. PET/CT scans comparing cell tracking with $^{111}\text{In}(\text{oxinate})_3$ (top) and $^{89}\text{Zr}(\text{oxinate})_4$ (bottom) labelled myeloma cells in mice. Cells initially accumulate in lungs, followed by migration to spleen, liver and bone marrow. Less uptake in kidney is observed for ^{89}Zr , suggesting greater stability and cell survival.²⁴

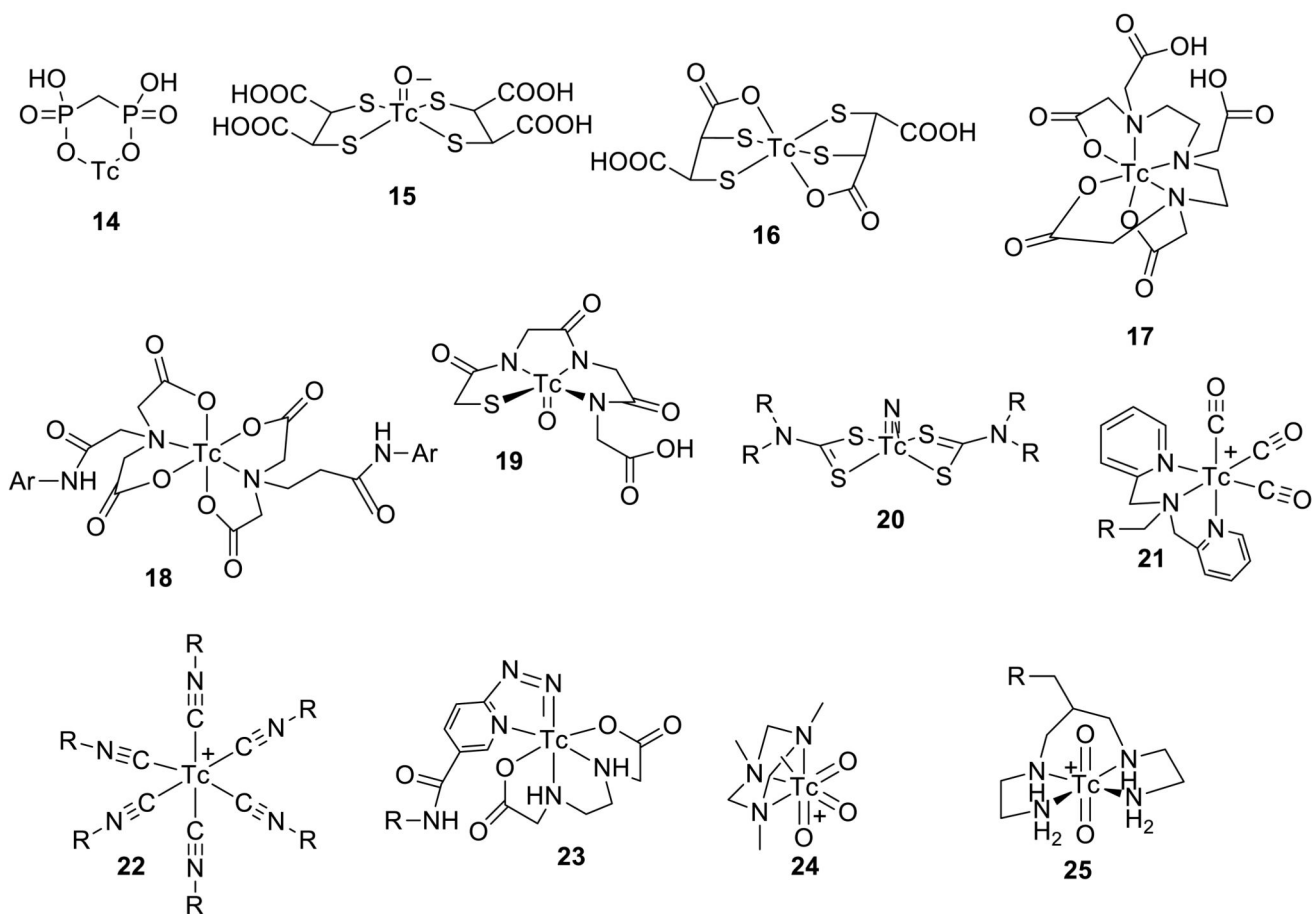


Figure 8.

A selection of established $^{99\text{m}}\text{Tc}$ radiopharmaceuticals and core structures (if known): TcMDP (**14**), Tc(V)DMSA (**15**), TcDMSA (**16**), TcDTPA (**17**), TcHIDA (**18**), TcMAG3 (**19**), Tc(V)-nitridobis(dithiocarbamate) (**20**), Tc(I)-tricarbonyl (**21**), Tc(I)-hexakis(isonitrile) (**22**), Tc(V)-hynic (**23**), Tc(VII)-trioxo (**24**), and Tc(V)-dioxo (**25**). Structures of **15**, **19**, **20**, **21**, **22**, **24** and **25** are known and well defined; the others are not clearly defined.

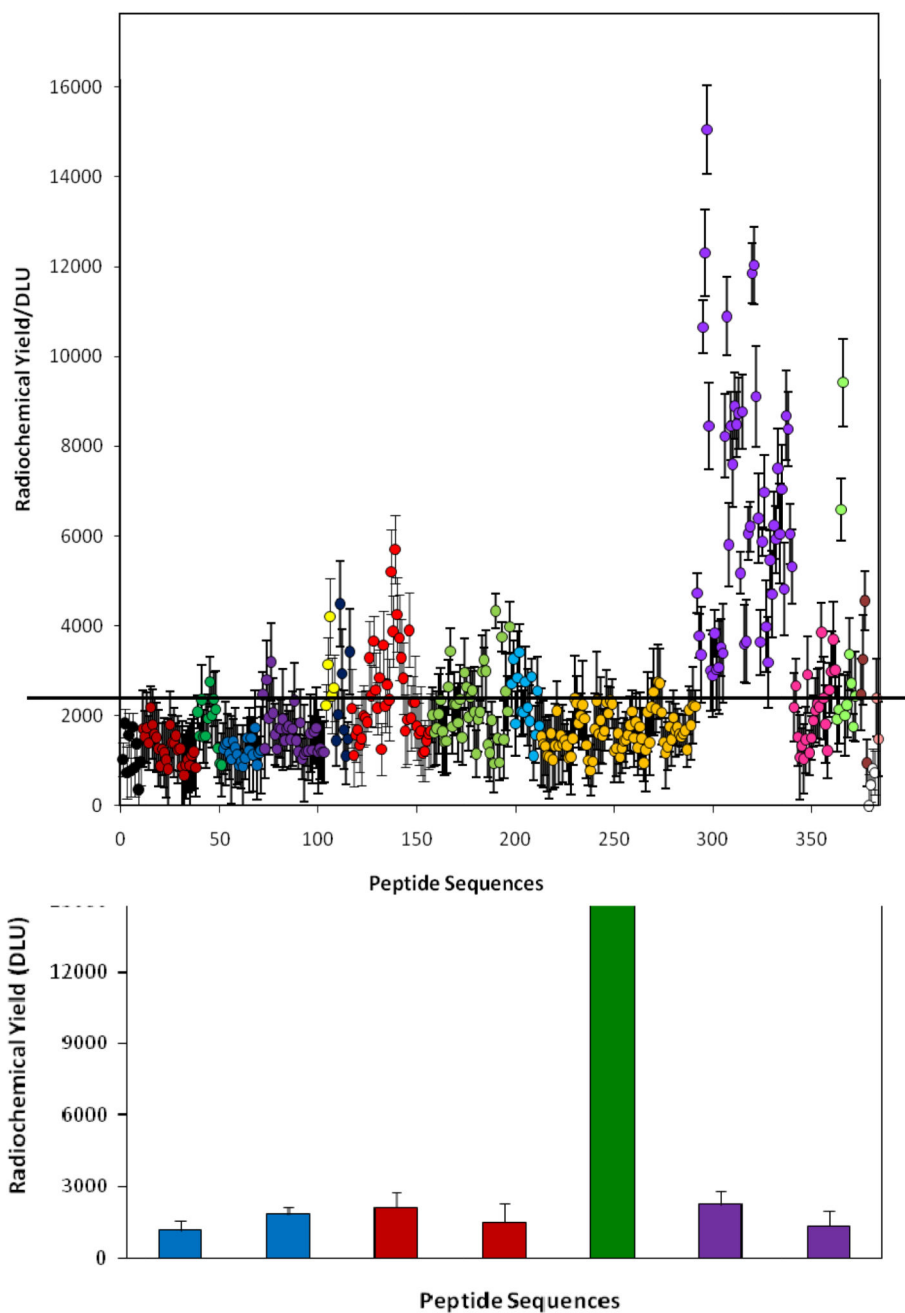


Figure 9. Optimisation of His-tag sequences for ^{99m}Tc tricarbonyl labelling from high throughput screening. Top: relative labelling efficiency of a range of peptides. Purple symbols represent His-tags with adjacent arginine or lysine residues (i.e. positively charged sequences). Other colours represent uncharged and negatively charged sequences. Bottom: Comparison of labelling efficiency of optimal binding sequence selected from the screening (green)53 with established his tags sequences.48–50

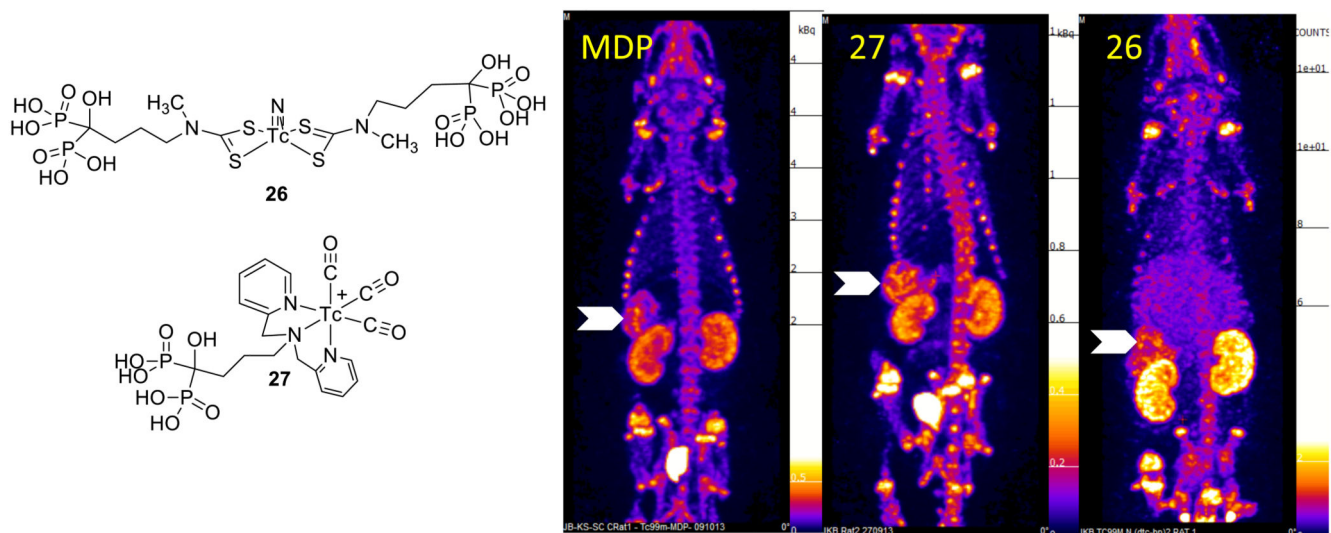


Figure 10. SPET images (maximum intensity projection) of vascular calcification in a mouse model 30 min after injection with [^{99m}Tc]-MDP, [^{99m}Tc]-**27** and [^{99m}Tc]-**26**. Arrows indicate uptake in calcified mesenteric arteries. Uptake in bone and clearance via kidneys and bladder is also evident.

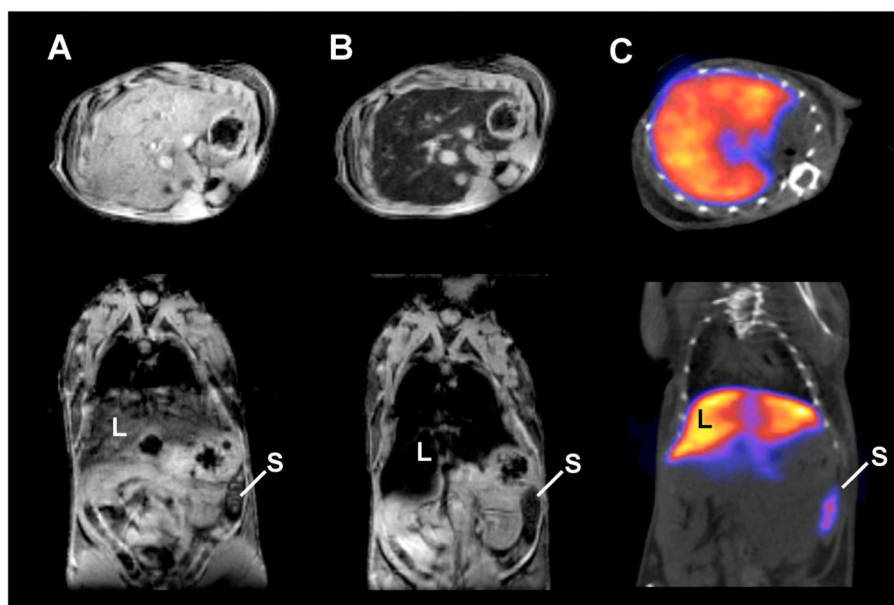
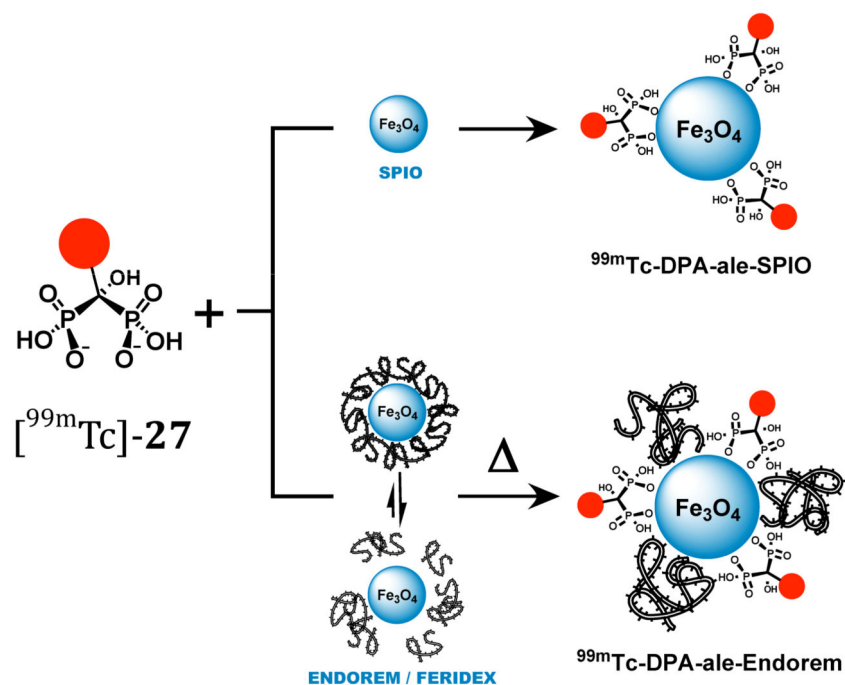
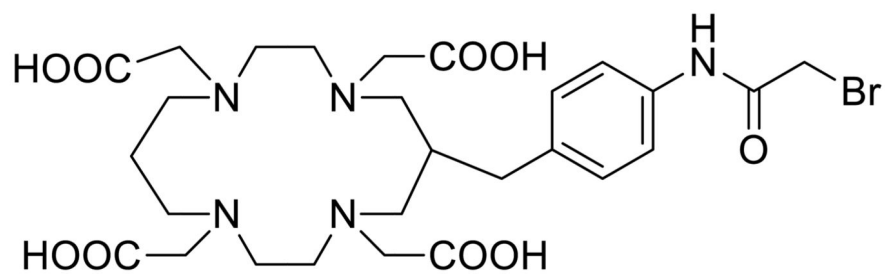
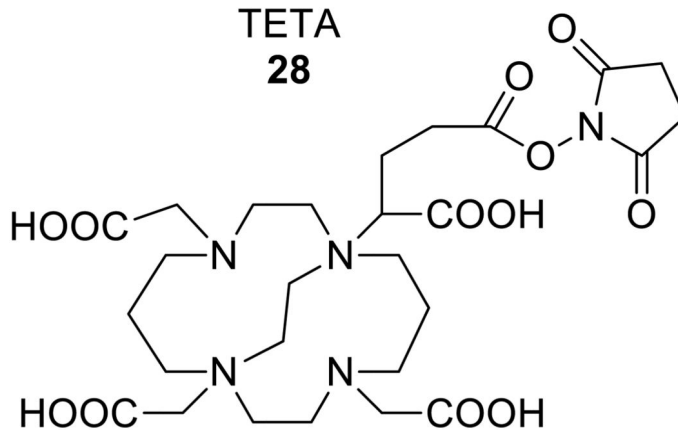


Figure 11.

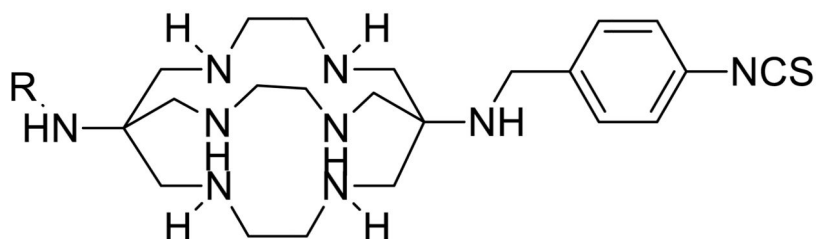
Dual-modality (MRI/SPET) contrast agent combining iron oxide nanoparticles with ^{99m}Tc radiolabel linked to the inorganic iron oxide surface via bisphosphonate groups. Top: assembly of composite particle; bottom: Mouse images, transverse sections through liver. A: MR image pre-injection of contrast agent; B: MR image post-injection of contrast agent showing darkening of liver due to accumulation of iron oxide nanoparticles; C: SPET/CT image showing co-localisation of ^{99m}Tc with iron oxide contrast in liver (L) and spleen (S).



TETA
28



CB-TETA
29



SarAr-NCS
30

Figure 12. Selection of chelators for radioisotopes of Cu^{2+} ; others of significance include **1** and **5** from Fig. 4.

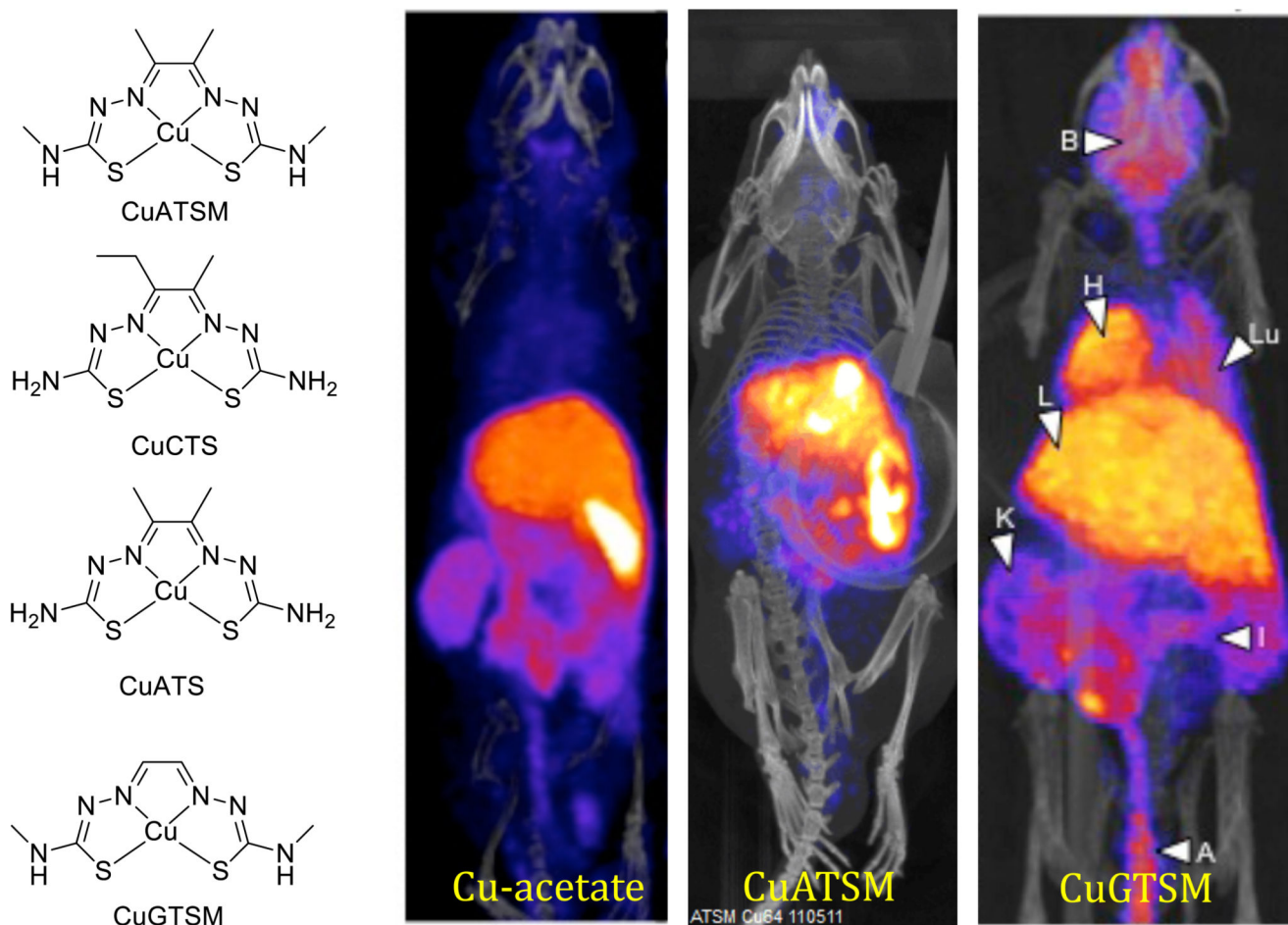
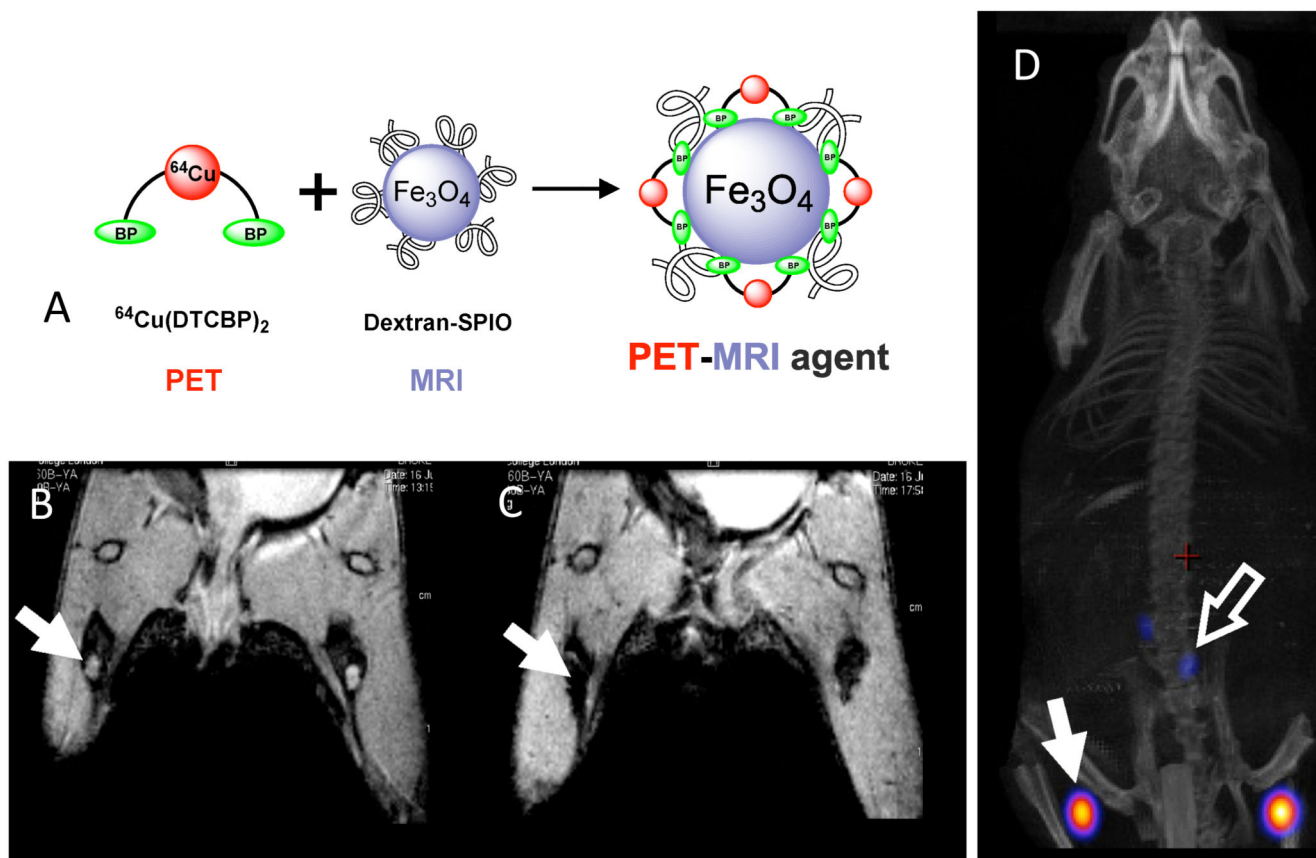
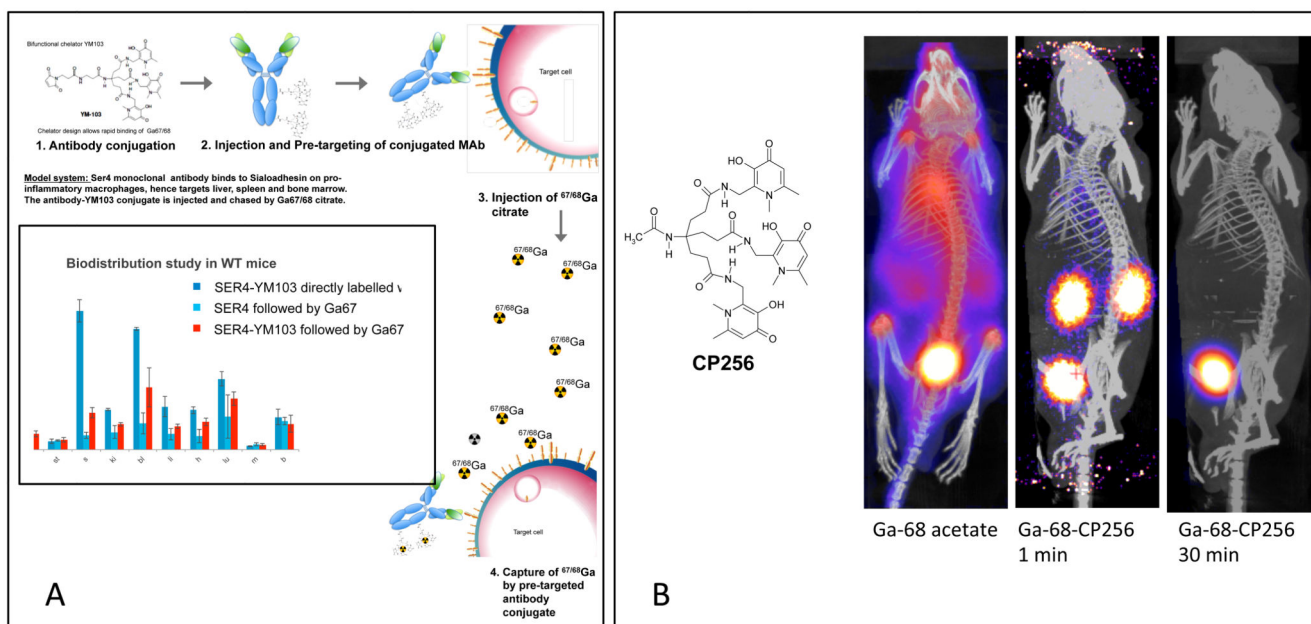


Figure 13. Structures of copper bis(thiosemicarbazone) complexes and PET imaging with ^{64}Cu and its bis(thiosemicarbazone) complexes in mice 30 min post injection. Cu-acetate is rapidly taken up in liver and excreted into the gut; CuATSM (hypoxia-selective tracer) behaves in a superficially similar way; CuGTSM (non-hypoxia-selective tracer) likewise shows liver and gut activity but also shows high uptake in normal brain and myocardium.

**Figure 14.**

Dual modality (PET/MR) imaging of sentinel lymph nodes in mice. A: assembly of ^{64}Cu -labelled iron oxide/dextran nanoparticles using a dithiocarbamate-bisphosphonate ligand (as used in technetium complex **26**, see Fig. 10). B: MR scan (coronal section) of hind limbs and lower abdomen, pre-injection of contrast agent. Lymph nodes are visible as bright areas (arrow). C: MR scan post-injection of contrast agent, showing darkening of lymph nodes due to uptake of MR contrast. D: PET/CT scan showing radioactivity co-localised with magnetic particles (arrows). The radioactivity remains bound to the magnetic particles *in vivo*.

**Figure 15.**

A. Concept of pre-targeting by *in vivo* transchelation of ⁶⁸Ga, which is feasible with YM103 (4 in Fig. 4) because of its ability to transchelate Ga³⁺ from transferrin in plasma and *in vivo*. Inset: Uptake of ⁶⁸Ga in most organs (including spleen which is the location of the macrophages expressing sialoadhesin, the SER4 antibody target) when given as a chase after administration of antibody-YM103 conjugate, is intermediate between that of the pre-labelled antibody and the distribution of ⁶⁸Ga given as a chase after administration of unconjugated antibody. The exception is bone, which is the target of unchelated ⁶⁸Ga (see part B, left image). This suggests that ⁶⁸Ga is able to find and bind to the pre-targeted antibody-YM103 conjugate *in vivo*. B: Demonstration that the tris(hydroxypyridinone) chelator CP256 (non-derivatised form of YM103) can bind to ⁶⁸Ga *in vivo* and excrete it rapidly via kidney. Left: Biodistribution of ⁶⁸Ga administered in unchelated form; centre and right: biodistribution of ⁶⁸Ga-CP256 complex 1 min and 30 min post-injection respectively, showing rapid renal excretion in progress and completed. Similar images are obtained if the ⁶⁸Ga is administered first, followed by the CP256 ligand.

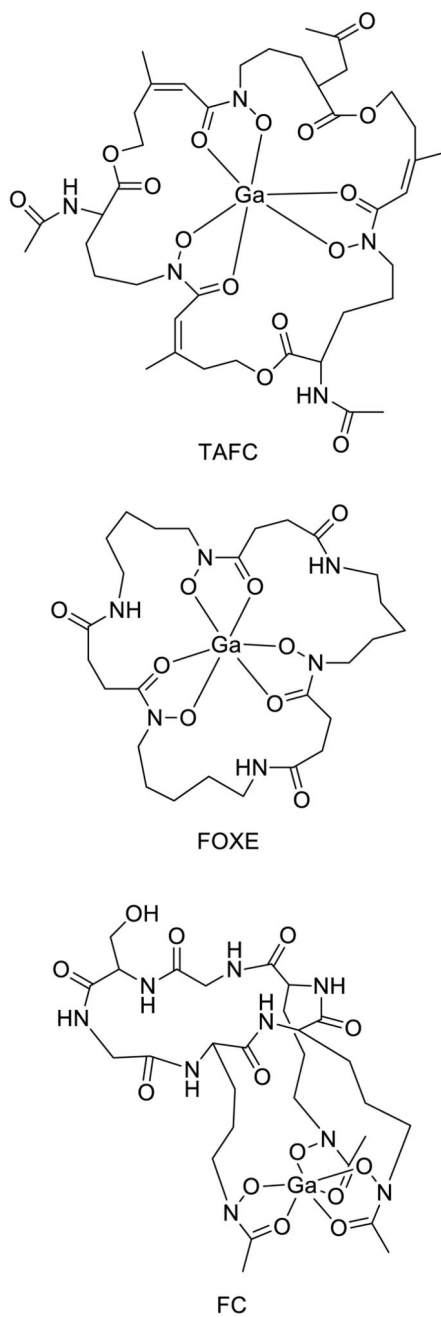


Figure 16. Siderophores labelled with ^{68}Ga for targeting microorganisms: TAFC = triacetylfusarinine; FOXE = ferrixoamine E; FC = desferriferricrocin.

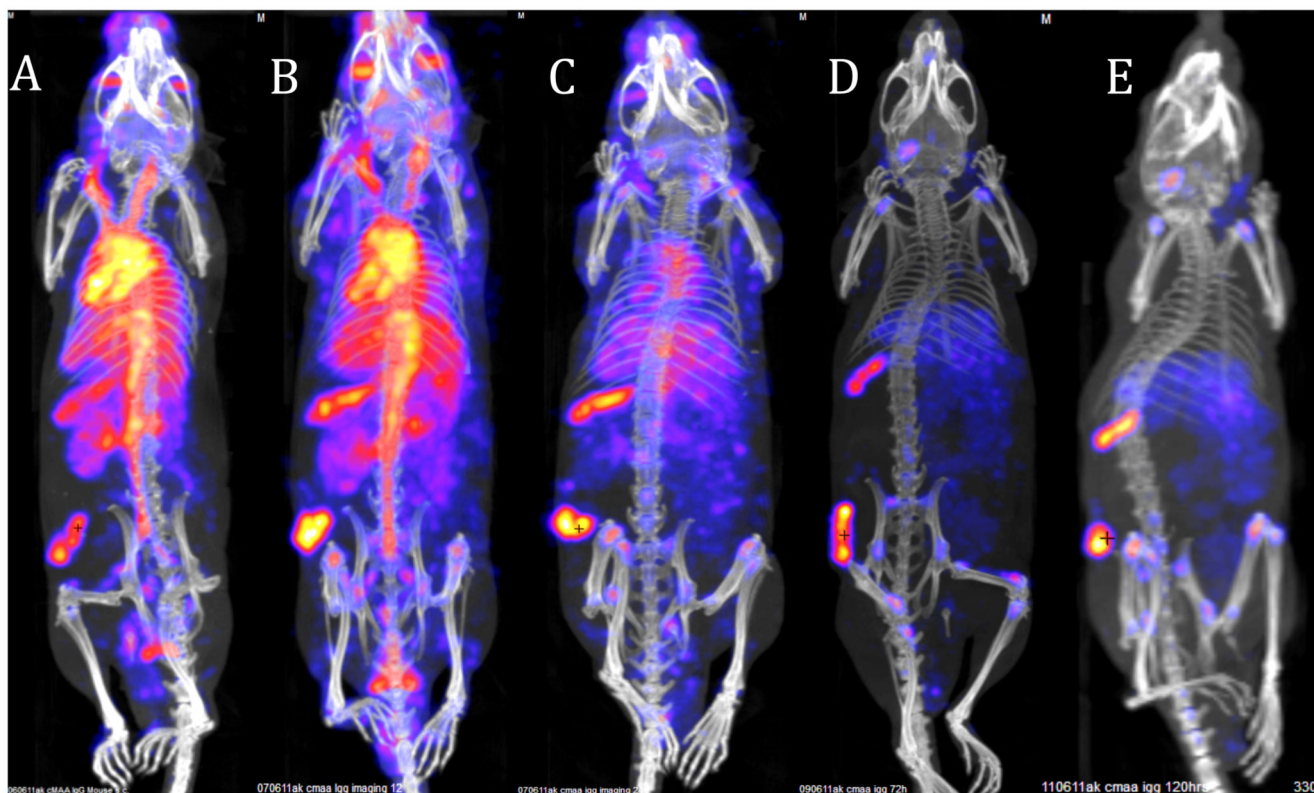


Figure 17.

Typical tumour SPET/CT imaging with whole IgG monoclonal antibody in mouse bearing an experimental melanoma on the flank, illustrating the need for long half-life radionuclide (in this case ^{111}In , half-life 2.8 days). CSPG4 IgG antibody, which binds to melanoma associated antigen, was labelled with ^{111}In using the bifunctional chelator CHX-A''-DTPA. Images show predominantly blood pool at 4 h (A) and 24 h (B) with increasing tumour- and spleen-to-blood ratio 48 h and optimal images are not seen until 48-120 h.

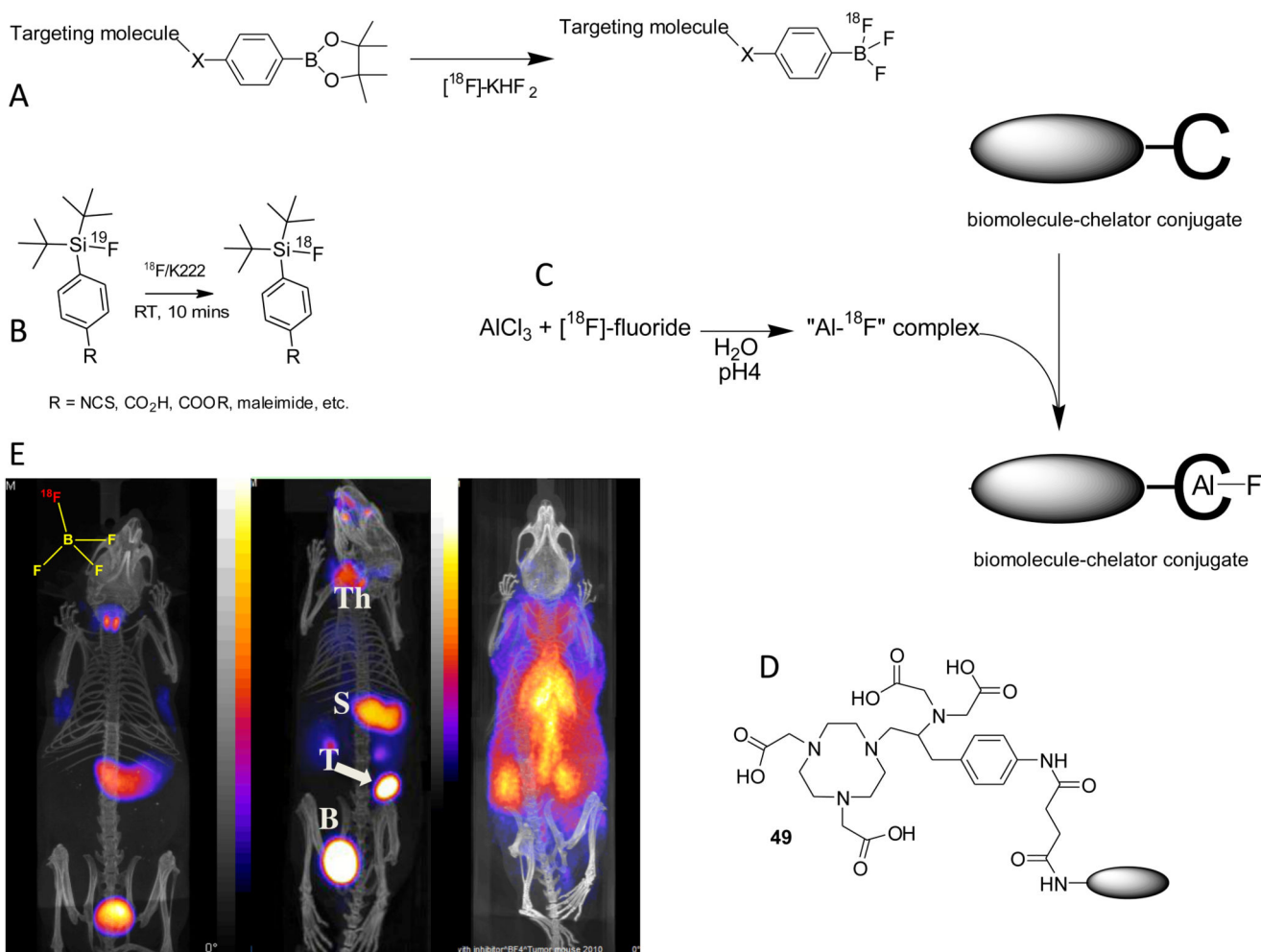


Figure 18.

A. Nucleophilic radiolabelling of boronic ester prosthetic group; B: Isotopic exchange labelling of fluorosilane prosthetic group; C: Use of coordinatively unsaturated aluminium complex as a binding site for fluoride ions in biomolecule labelling; D: currently favoured ligand for chelation of Al^{3+} and labelling with $[^{18}\text{F}]\text{-fluoride}$; E: PET-CT imaging of sodium/iodide symporter (NIS) activity mouse using NIS substrate $[^{18}\text{F}]\text{-BF}_4^-$, 30 min post-injection. Left: normal mouse showing thyroid and stomach uptake and excretion into bladder; Centre: mouse with implanted NIS-expressing breast tumour showing tumour (T) uptake as well as thyroid (Th) and stomach (S) uptake; right: normal mouse pre-injected with perchlorate to block NIS activity, showing radioactivity largely confined to blood pool.

Table 1
Copper radioisotopes available for PET and radionuclide therapy. EC = electron capture.

Isotope	β^- %, E_{ave}	β^+ , %, E_{ave}	other	$t_{1/2}$
Cu-60		93%, 0.87 MeV	EC	24 min
Cu-61		62%, 0.53 MeV	EC	3.33 h
Cu-62		98%, 1.32 MeV	EC	9.75 min
Cu-64	39%, 0.19 MeV	18%, 0.28 MeV	EC	12.7 h
Cu-67	100%, 0.12 MeV		γ , 93 KeV, 52%	62 h